

STAT3 but not STAT5 contributes to the protective effect of electro-acupuncture against myocardial ischemia/reperfusion injury

Hui-Hui Guo^{1#}, Xin-Yue Jing^{1#}, Hui Chen², Hou-Xi Xu¹, Bing-Mei Zhu^{3*}

1 Key Laboratory of Acupuncture and Medicine Research of Ministry of Education, Nanjing University of Chinese Medicine, Nanjing, 210023, Jiangsu, China;

2 Rehabilitation Medicine Department, YEDA Hospital of Yantai, Yantai, 264000, Shandong, China;

3 Regenerative Medicine Research Center, West China Hospital, Sichuan University, Chengdu, 610041, Sichuan, China.

These authors have equal contribution

*Corresponding author

Prof. Bing-Mei Zhu

Present address: Regenerative Medicine Research Center, West China Hospital, Sichuan University, Keyuan Road 4, Gaopeng Street, Chengdu, Sichuan, P.R.China. 610041

Tel: +86-28-85164069(O)

Fax:+86-28-85164037

e-mail: zhubm64@hotmail.com

Keywords

Myocardial ischemia reperfusion (I/R) / STAT5/ STAT3/ Electro-acupuncture/ Cardioprotection

The total number of words : 9802

Abstract

Late remote ischemia preconditioning (RIPC) and electro-acupuncture (EA) have both been suggested to reduce injury caused by myocardial ischemia/reperfusion (I/R). Our previous study has found that cardioprotection in RIPC is STAT5-dependent. Here, we aim to observe the effects of electro-acupuncture pretreatment (EAP) on I/R in the presence or absence of STAT5 in mice and investigate whether the protection of EAP is in a STAT5-dependent manner. In this study, EAP decreased myocardial infarction size (IS) /total area (TA) and rate of cardiomyocyte apoptosis. STAT5 was activated by EAP in the *Stat5^{fl/fl}* mice but not in the *Stat5-cKO* mice, whereas, STAT3 was activated by EAP only in the *Stat5-cKO* but not in the *Stat5^{fl/fl}* mice. Differentially expressed genes (DEGs) regulated by EAP in the *Stat5^{fl/fl}* and the *Stat5-cKO* mice were quite distinct, indicating that EAP may activate IL-6/STAT3 signal in the absence of *Stat5*, and that EAP-induced cardioprotection against myocardial I/R injury was correlated with the activation of anti-apoptotic signaling and cardiomyocyte-survival signaling. Our results, for the first time, demonstrated that the protective effect of EAP was attributed to, but not dependent on, STAT5.

Introduction

It is known that myocardial ischemia/reperfusion (I/R) injury is a pathological phenomenon that can cause further cardiomyocyte death following blood restoration (Li *et al*, 2019; Chen *et al*, 2019). Remote ischemic preconditioning (RIPC) has been demonstrated as an intervention to attenuate ischemic-reperfusion (I/R) injury and protect myocardium for many years (Davidson *et al*, 2019; Ekeloef *et al*, 2019; Cho & Kim, 2019; Heusch, 2015). Our recent study has shown that signal transducer and activator of transcription 5 (STAT5) plays a critical role in RIPC, and RIPC mediates cardioprotection by activating anti-apoptotic and cardiomyocyte-survival signaling in a STAT5-dependent manner (Chen *et al*, 2018). Electro-acupuncture (EA), as one of the Traditional Chinese Medicine (TCM) approaches, has been applied to treat many diseases clinically around the world (Painovich & Longhurst, 2015). Increasing experimental and clinical evidences have confirmed EA's effectiveness on cardiovascular diseases (Zhang *et al*, 2020; Ji *et al*, 2018; Huang *et al*, 2014; Fu *et al*, 2014; Zeng *et al*, 2018; Lu *et al*, 2016). A very recent article (Zhao *et al*, 2019) collected a total of 1651 patients with chronic stable angina and performed a clinical trial with acupuncture treatment. This study has shown that acupuncture as an auxiliary treatment method can alleviate clinical pain in patients with chronic stable

angina, reduce the patient's anxiety and depression, and eventually improve the quality of life for these patients. Its underlying mechanisms have been known, include anti-apoptosis and anti-oxidative stress, as well as reducing inflammatory damage, calcium overload, and endoplasmic reticulum stress (Chen *et al*, 2019; Tang *et al*, 2019).

Studies, including our previous work, have shown that using electro-acupuncture before the event of ischemia-reperfusion, which is also called electro-acupuncture pretreatment (EAP), could protect cardiomyocytes by reducing the myocardial infarct size and regulating some molecular signaling, such as apoptosis and survival signaling (Huang *et al*, 2014; Lu *et al*, 2016). Given that the main molecule involved in RIPC in human patients is STAT5 (Cheung *et al*, 2006; Chen *et al*, 2018), we question whether EAP can also protect myocardium against ischemia-reperfusion through STAT5 signaling pathway. Therefore, we have employed the cardiomyocyte-specific *Stat5* knockout (*Stat5-cKO*) mice and generated myocardial I/R model. EA is applied to the mice seven days before the I/R surgery. This study will determine whether EAP shares the same mechanism with RIPC and plays a preconditioning-like role as RIPC does on I/R injury. We have also carried on a genome-wide gene profiling to further find more candidate genes involved in the cardioprotection that results from EAP.

Results

1. EAP reduced myocardial infarct size and attenuated cardiomyocytic apoptosis to the same extent in both the *Stat5^{fl/fl}* mice and the *Stat5-cKO* mice

We did not observe any difference in the daily behavior and cardiac performance between the *Stat5^{fl/fl}* mice and the *Stat5-cKO* mice, same as seen in our previous study (Chen *et al*, 2018). EA pretreatment was applied on PC6 acupoints in both *Stat5^{fl/fl}* mice and *Stat5-cKO* mice for seven days before they received myocardial I/R surgery. We did not see any difference before or after EAP in their daily behavior and cardiac performance between these two genotypes. We then harvested the heart tissues after I/R and measured myocardial infarct areas by TTC staining (Fig 1) and found that EAP significantly reduced infarct size in the *Stat5^{fl/fl}* mice ($44.6 \pm 1.3\%$ without EAP vs. $31.2 \pm 5.1\%$ with EAP, $P < 0.05$) and the *Stat5-cKO* mice ($41.9 \pm 4.1\%$ without EAP vs. $31.3 \pm 4.5\%$ with EAP, $P < 0.05$). There was no significant difference between the *Stat5^{fl/fl}*+EA+I/R and the *Stat5-cKO*+EA+I/R mice.

TUNEL staining was performed to detect apoptosis in the myocardial cells. As

shown in Fig 2, the *Stat5^{fl/fl}*+EA+I/R group had fewer TUNEL positive cells compared to the *Stat5^{fl/fl}*+I/R group ($P < 0.01$). Likewise, the apoptotic myocardial cells were also significantly reduced in the *Stat5-cKO*+EA+I/R group compared to the *Stat5-cKO*+I/R group ($P < 0.01$).

Figure 1.

Figure 1. Acupuncture reduced myocardial infarct size.

A TTC staining was used to measure ischemic infarct area.

B The ratio of infarct size/ total area was calculated and presented as percentage.

Data information: In B, data are presented as mean \pm SEM, data were analyzed by one-way ANOVA with Tukey's post hoc correction. Normal tissues are red, and ischemic infarct areas are pale white. * $P < 0.05$, compared with *Stat5^{fl/fl}*+I/R group, # $P < 0.05$, compared with *Stat5-cKO*+I/R group.

Source data are available online for this figure.

Figure 2.

Figure 2. Effects of EAP on apoptosis of myocardial tissues in the *Stat5^{fl/fl}* and the *Stat5-cKO* mice.

A,B The apoptosis index was measured by TUNEL staining.

Data information: Values are mean \pm SEM, n = 5. ** $P < 0.01$, compared with the *Stat5^{fl/fl}*+I/R group, ## $P < 0.01$, in comparison with the *Stat5-cKO*+I/R group.

2. EAP activated STAT5 in the *Stat5^{fl/fl}* mice but not in the *Stat5-cKO* mice under myocardial I/R condition

To further explore whether the myocardial protection of EAP against I/R injury is STAT5 dependent, we examined protein levels of p-STAT5 in the heart tissues by western blotting. While EAP markedly increased p-STAT5/GAPDH in the *Stat5^{fl/fl}* mice compared with the *Stat5^{fl/fl}* mice subjected to I/R, EA had no effect on STAT5 activation in the hearts of the *Stat5-cKO* mice (Fig 3A and B). This suggests that STAT5 may participate in the process of EAP protection against myocardial I/R injury.

Figure 3.

Figure 3. EAP activated STAT5 protein in the heart tissues of the *Stat5^{fl/fl}* but not the *Stat5-cKO* mice.

A The images of representative western blotting.

B Quantitative analysis of p-STAT5 protein in each group.

Data information: In B, data are presented as mean \pm SEM, data were analyzed by two-way ANOVA, Bonferroni's multiple comparison test, n=8. ** $P < 0.01$, compared with the *Stat5^{fl/fl}*+I/R group, # $P < 0.05$, in comparison with the *Stat5-cKO*+I/R group.

3. IL-6/gp130/STAT3 signaling was activated by EAP in the absence of *Stat5*

As described in our previous study (Chen *et al*, 2018) and shown in our current observation, STAT5 is a very important molecule in myocardial protection through RIPc or EAP against I/R injury. However, EAP did also display a protective role against myocardial I/R injury when STAT5 was absent in the mouse heart, suggesting that the EAP-induced myocardial protection may be STAT5-independent and some other proteins may be in charge of this function when STAT5 is missing. Considering the possibility of compensation by STAT3, we then evaluated the expression levels of STAT3 protein and p-STAT3 protein in the heart tissues of both *Stat5^{fl/fl}* mice and *Stat5-cKO* mice. We discovered that the expression of p-STAT3 was increased in the *Stat5-cKO*+EA+I/R mice compared to the *Stat5-cKO*+I/R group, whereas this was not observed in the *Stat5^{fl/fl}* mice (Fig 4A). To understand the mechanism by which STAT3 was activated in this process, we further detected the upstream molecules of STAT3 and found that the mRNA level of IL-6 and gp130 were upregulated in the *Stat5-cKO*+EA+I/R mice compared to those in the *Stat5-cKO*+I/R mice, suggesting that EAP activated the IL-6/gp130/STAT3 pathway in the absence of *Stat5* gene when the heart was exposed to myocardial I/R damage, a process not seen in the presence of *Stat5* (Fig 4B).

Figure 4.

Figure 4. The expression of IL-6/gp130/STAT3 axis related molecules.

A The expression of STAT3 and p-STAT3 proteins was detected by western blotting.

B The expression of IL-6 and gp130 mRNAs was performed by RT-PCR.

Data information: ** $p < 0.01$, compared with the *Stat5^{fl/fl}*+I/R; ## $P < 0.01$, compared with the *Stat5^{fl/fl}*+EA+I/R; && $P < 0.01$, compared with the *Stat5-cKO*+I/R, n=4-6. B ** $P < 0.01$, compared with the *Stat5^{fl/fl}*+I/R group, # $P < 0.05$ compared with the *Stat5^{fl/fl}*+EA+I/R group, \$ $P < 0.05$ compared with the *Stat5-cKO*+I/R group, n=3-4.

4. Genome-wide analysis revealed gene expression profiles in both *Stat5^{fl/fl}* mice and *Stat5-cKO* mice with or without EAP followed by myocardial I/R injury

To find the candidate genes participating in the EAP-induced protection against myocardial I/R injury, RNAs were extracted from the heart tissues and RNA-seq was

performed using next generation high-throughput sequencing. With the Cufflinks package, we filtered out the top 30 differentially expressed genes (DEGs) by fold changes through comparing the *Stat5^{fl/fl}*+I/R group with the *Stat5^{fl/fl}*+EA+I/R group and the *Stat5-cKO*+I/R group with the *Stat5-cKO*+EA+I/R group (Table 1A and B). First, we compared DEGs between the *Stat5^{fl/fl}*+I/R group and the *Stat5^{fl/fl}*+EA+I/R group and between the *Stat5-cKO*+I/R group and the *Stat5-cKO*+EA+I/R group. Venn diagrams were drawn based on the list of filtered DEGs among four groups (Fig 5). The results showed that, compared with the *Stat5^{fl/fl}*+I/R group, 1052 genes were differentially expressed in the *Stat5^{fl/fl}*+EA+I/R group, and 1039 DEGs were obtained by comparing the *Stat5-cKO*+I/R group and the *Stat5-cKO*+EA+I/R group, in which 133 genes were overlapped by these two clusters. Among these 4 groups, only two genes, *Hspa1a* and *Pttg1* were found to belong to all four groups, suggesting that STAT5-dependent genes and EAP-regulated genes were located in different categories. We further analyzed these genes and further tried to understand mechanisms by which myocardial I/R pathology occurs in the presence or absence of *Stat5* and how EAP protects myocardial I/R injury through regulating gene expressions. We found that among the EAP up-regulated genes and down-regulated genes in the presence of STAT5 (*Stat5^{fl/fl}*+I/R vs *Stat5^{fl/fl}*+EA+I/R), lots of genes (such as *Fosb*, *Fos*, *Cxcl5*, *Cxcl*, *Egr1*, *Egr2*, *Nr4a3*, *Socs3*, *Ccn5*, *Myl4*, *Zhx2*, *Dkk3*, and *Dynl1l1*) have been reported to participate in the protection against the myocardium ischemia, I/R, cardiac hypertrophy or hypoxia in the literatures (Wu *et al*, 2017; Kubota *et al*, 2019; Wang *et al*, 2018; Sun *et al*, 2019; Ma *et al*, 2020; Oba *et al*, 2012; Tian *et al*, 2020; Stobdan *et al*, 2015; Bos *et al*, 2012; Zhai *et al*, 2018; El-Magd *et al*, 2017). These DEGs belong to many functional pathways, such as the JAK/STAT signaling pathway, the TNF signaling pathway, apoptosis, or the NF-kappa B signaling pathway. In the other hand, when STAT5 is absent, we found that among the top 30 DEGs generated by comparing the *Stat5-cKO*+EA+I/R group with the *Stat5-cKO*+I/R group (Table 1B), *Rps6*, *Mmp3*, *pttg1*, *Rac2* had a strong relationship with the IL-6/STAT3 signaling pathway, as reported previously in the literatures (Dern *et al*, 2019; Wu *et al*, 2020; Calamaras *et al*, 2015; Sharma *et al*, 2019; Abilleira *et al*, 2006; Zhu & Sun *et al*, 2017; Huang *et al*, 2018; Lai *et al*, 2017; Shirakawa *et al*, 2018; Wen *et al*, 2015).

Figure 5.

Figure 5. Venn diagrams and clustering analysis of RNA-seq results.

Data information: Venn diagrams were drawn based on our RNA-seq data sets. Blue circle indicates the numbers of genes up- and down-regulated in the *Stat5^{fl/fl}*+EA+I/R group (vs. the *Stat5^{fl/fl}*+I/R group); pink circle represents the numbers of up- or down-regulated genes in the *Stat5-cKO*+EA+I/R group (vs. *Stat5-cKO*+I/R group). 133 genes were overlapped by these two clusters.

To further understand the potential pathways involved in the STAT5-related DEGs and the EAP-modified DEGs under I/R, we then carried out pathway analyses for these DEGs. Encyclopedia of Genes and Genomes (KEGG) pathway analyses were performed using DAVID Bioinformatics Resources, and the top 20 pathways were outlined in Fig 6.

Figure 6.

Figure 6. KEGG pathway analysis of up- and down-regulated genes in the heart tissues in the presence or absence of *Stat5* (A–C).

A The top 20 KEGG pathways were drawn from the 919 DEGs genes by comparing the *Stat5^{fl/fl}*+I/R group and the *Stat5^{fl/fl}*+EA+I/R group shown in Figure 5.

B The top 20 KEGG pathways were drawn from the 906 DEGs genes by comparing *Stat5-cKO*+I/R group and *Stat5-cKO*+EA+I/R group shown in Figure 5.

C The top 20 KEGG pathways were drawn from the 133 co-regulated genes shown in Figure 5.

KEGG pathway analyses suggested that, in the presence of *Stat5*, EAP-activated genes were mainly enriched in the JAK-STAT signaling pathway, the TNF signaling pathway, cytokine-cytokine receptor interaction, the IL-17 signaling pathway, the NF-kappa B signaling pathway, and the MAPK signaling pathway (Fig 6A). They may work together to protect the myocardium from I/R injury (Castejon *et al*, 2019; Yuan *et al*, 2019; Świerkot *et al*, 2015). In contrast, in the *Stat5-cKO* mice, the myocardial protection of EAP mainly concentrated in Ribosome pathways, thermogenesis, and the oxidative phosphorylation pathway (Fig 6B). Moreover, we also analyzed the top 20 KEGG pathways of the 133 overlapped genes (Fig 6C), showing that the EAP-regulated part of the STAT5-independent genes were mainly located in inflammation related pathways (such as the IL-7 signaling pathway, human T-cell leukemia virus 1 infection, antigen processing and presentation, and the TNF signaling pathway).

Table 1.

5. Apoptotic and survival signaling were regulated by EAP only in the presence of STAT5.

Based on the above genome-wide profiling data, we detected that EAP could activate apoptotic and survival signaling in mice with I/R injury. To further validate these findings, we studied apoptotic and survival related protein expression in myocardial tissues of the *Stat5^{fl/fl}* and the *Stat5-cKO* mice with EAP. The results showed that the expression of Bcl-2 and Bcl-xL were significantly increased in the *Stat5^{fl/fl}*+EA+I/R group compared with the *Stat5^{fl/fl}*+I/R group ($P < 0.05$), whereas the expression of Cyt C did not change between these two groups (Fig 7). In contrast, we did not detect significant differences in these protein expressions in the hearts of *Stat5-cKO* mice, with or without EAP, suggesting that STAT5 is required for regulating anti-apoptotic signaling induced by the EAP stimulus. We then detected the level of IL-10, an important cytokine in cardio-protection, and its related proteins, PI3K, AKT, and p-AKT (Fig 8). The results showed that IL-10 and p-AKT were elevated by EAP in the presence but not absence of STAT5, however IL-10 was up-regulated in the hearts of both *Stat5^{fl/fl}* mice and *Stat5-cKO* mice with EAP. These results indicate that the protective effect of EAP against myocardial I/R injury in survival signaling is partially STAT5-dependent.

Figure 7.

Figure 7. The expression of apoptosis-related proteins.

A,B Western blotting was used to detect the level of Bcl-2, Bcl-XL and Cyt C in each group.

Data information: ** $P < 0.01$, compared with *Stat5^{fl/fl}*+I/R group, n=6.

Figure 8.

Figure 8. The expression of survival signaling-related proteins.

A,B Western blotting was used to detect the level of IL-10, p-AKT, and AKT in each group.

Data information: * $P < 0.05$, compared with *Stat5^{fl/fl}*+I/R group, # $P < 0.05$, in comparison with *Stat5-cKO*+I/R group, n=6.

Discussion

Ischemic heart disease is still the major cause of premature mortality and disability worldwide (Gupta & Wood, 2015). As a clinically effective method against myocardial I/R injury, early coronary reperfusion reduces the infarct size, but reperfusion by revascularization initiates a cascade of events that can accelerate and

extend post-ischemic injury (Binder *et al*, 2015; Yellon & Hausenloy, 2017). Remote ischemia preconditioning (RIPC) has been confirmed to be an effective and clinically applicable perioperative method to reduce the risk of myocardial injury (Hausenloy *et al*, 2019; Ekeloef *et al*, 2019). In our previous study, we have found that STAT5 plays a key role in the RIPC-mediated late cardio-protection through anti-apoptotic signaling and the PI3K/AKT survival pathway (Chen *et al*, 2018). Similar to RIPC, EA pretreatment at acupoint PC6 like a late stimulating can also protect myocardium under certain disease conditions by stimulating multiple functional pathways.

In the present study, we explored the role of STAT5 in EAP-induced myocardial protection against ischemia-reperfusion by employing cardiomyocyte-specific *Stat5-cKO* mice. We observed that EAP could reduce the infarct size and myocardial cell apoptosis in both *Stat5^{fl/fl}* and *Stat5-cKO* mice (Fig 1 and Fig 2), suggesting that STAT5 is not required in the cardioprotection of EAP against myocardial I/R injury. To understand how EAP played a protective role in the loss of *Stat5*, we performed RNA sequencing with the I/R injured heart tissue. We found that EAP can increase the mRNA expressions of *Fosb*, *Fos*, *Cxcl5*, *Cxcl1*, *Egr1*, *Egr2*, *Nr4a3*, and *Socs3*, which were reported to be involved in anti-apoptosis, anti-inflammation, antioxidation, and STAT3/5 signaling when STAT5 is intact. *Fosb* and *Fos*, as two components of AP-1, can protect against myocardial I/R injury via anti-apoptosis, anti-oxidative stress, and anti-inflammatory activation (Wingelhofer *et al*, 2018; Walker *et al*, 2014; Walker *et al*, 2013). *Cxcl5* and *Cxcl1* are two members in the CXC family of chemokines and have been shown to improve cell survival after myocardial injury through the promotion of wound healing by changing neutrophil infiltration and activating the phosphatidylinositol 3-kinase pathway (Cai *et al*, 2020; Zhou *et al*, 2020). *Egr1* and *Egr2* belong to early growth response protein 1/2. They can induce myocardial injury by regulating myocardial autophagy, cell death, and the progression of myocardial fibrosis (Wang *et al*, 2018; Cao *et al*, 2010). *Nr4a3*, a member of the NR4A orphan nuclear receptor, plays a protective role during acute myocardial infarction by suppressing inflammatory responses via the JAK2-STAT3/NF- κ B pathway (Obana *et al*, 2010; Walker *et al*, 2014). *Socs3*, a negative effector of STAT3 signaling, is an NF- κ B/IKK-induced gene. IKK-mediated NF- κ B activation can coordinately illicit negative effects on STAT signaling (Gopinath, 2017). Aside from the above up-regulated genes, *Hspa1a* and *Hspa1b* are also important factors during the restoration of myocardial I/R injury (Jiang *et al*, 2014; Wilhide *et al*, 2011) and

appear to be up-regulated by EAP. In addition, among the down-regulated DEGs, *Ccn5* is an anti-hypertrophic and anti-fibrotic factor during adverse cardiac remodeling. It can be regulated by activating JAK/AKT/STAT3-signaling in luminal-type (ER-positive) breast cancer (BC) cells (Haque *et al*, 2018). *Myl4* (myosin light polypeptide 4) is a key gene for atrial contractile, electrical, and structural integrity (Udoko *et al*, 2016). *Zhx2*, as one of the transcription factors, can improve macrophage survival and pro-inflammatory functions in atherosclerotic lesions (Tian *et al*, 2020; Alfonso-Jaume *et al*, 2006). *Hic1*, a transcriptional repressor that modulates the expression of cell-cycle genes, can affect heart function and be regulated by the IL-6/STAT3 pathway (Wen *et al*, 2019; Sulston *et al*, 2017). *Gas1*, *pttg1*, *Nrtn*, and *Tnfrsf25* have also been identified as key molecules in the heart tissue by regulating tissue formation, metabolism, apoptosis of cardiomyocytes, and the interaction of cytokine-cytokine receptor in the JAK/STAT pathway (Tang *et al*, 2019; Jiang *et al*, 2019; Saddic *et al*, 2018).

In short, many of the genes and pathways found in our RNA-seq have been attributed to MI or I/R injury and are regulated by EAP in the *Stat5^{fl/fl}* mice. This indicates that EAP can mimic RIPC and play a protective role against I/R injury by altering functional gene expression in the presence of STAT5.

Intriguingly, in the *Stat5-cKO* mice, EAP regulated different DEGs, of which *Rps6*, *Mmp3*, *Pttg1*, and *Rac2* are involved in the IL-6/STAT3 signaling pathway. In addition, ribosomal, thermogenesis, and oxidative phosphorylation pathways are activated by EAP in the absence of STAT5. Among these DGEs, *Mmp3*, known as matrix metalloproteinase 3, encodes a member of the matrix metalloproteinase family of the extracellular matrix-degrading enzymes that are involved in tissue remodeling, wound repair, progression of atherosclerosis, and tumor invasion (Abilleira *et al*, 2006). Recent findings indicate that the binding of STAT3 to the MMP promoter promotes the transcription of *Mmp3* gene, which accounts for IL-6-induced MMP gene activation (Zhu & Sun, 2017). Pituitary tumor transforming 1 (*pttg1*) has been reported as an oncogene that is originally cloned from rat pituitary tumor cells. Huang *et al*. have demonstrated that *pttg1* expression is regulated by IL-6 via the direct binding of activated STAT3 to the *pttg1* promoter in LNCa P cells. *Rac2*, one of the Rac family members, is expressed mainly in the hematopoietic cells (Huang *et al*, 2018). Rac protein can promote glioblastoma tumor sphere-induced angiogenesis in the zebrafish exnotransplantation model. Knockdown of Rac protein reduces the

tumorigenesis in the mouse model *in vivo* (Lai *et al.*, 2017). Lai *et al.* have detected reduced STAT3 activation in the Rac down-regulated glioblastoma cells without affecting STAT5 activation. Osteopontin (OPN) is also known as secreted phosphoprotein 1 (Spp1). High levels of intracellular galectin-3 expression are essential for transcriptional activation of Spp1 in STAT3-mediated polarization toward M2 macrophages after MI (Shirakawa *et al.*, 2018; Wen *et al.*, 2015). The phosphorylation sites of ribosomal protein S6 (Rps6) have been mapped to five clustered residues, which play an important role in protein synthesis in cardiac myocytes and cardiac function (Dern *et al.*, 2019; Wu *et al.*, 2020; Calamaras *et al.*, 2015; Sharma *et al.*, 2019).

Through RNA-seq profiling, we expect different mechanisms were involved in EAP protection against myocardial I/R injury between *Stat5^{fl/fl}* and *Stat5-cKO* mice. Combined with the molecular biological data in this study, these results support our hypotheses that EAP may activate STAT3 in the absence of STAT5 and function as a protective approach for I/R.

In fact, multiple studies have demonstrated that in the absence of a given STAT member, receptors will recruit other STAT members instead (Hennighausen *et al.*, 2018; Yu *et al.*, 2010; Valle & Soto *et al.*, 2020; Hosui *et al.*, 2009; Hin *et al.*, 2020; Friedbichler *et al.*, 2012). STAT5 and STAT3 are two proteins of STAT family that show high homology in their functional domains, can be activated by different mechanisms, and bind to distinct loci to regulate specific target gene expression (Wingelhofer *et al.*, 2018). STAT3 and STAT5 proteins can also bind to the same regulatory oncogenic loci, resulting in compensatory or antagonistic signaling (Walker & Xiang, 2014; Walker *et al.*, 2013). Nevertheless, the role of STAT5 and STAT3 in myocardial I/R injury by EAP have not been studied yet. Interestingly in our study, p-STAT3 protein has significantly increased in the *Stat5-cKO*+EA+I/R group compared to the *Stat5^{fl/fl}*+EA+I/R group (Fig 4), suggesting that EAP activates STAT3, which then contributes to protecting the myocardium against I/R injury in the *Stat5-cKO* mice. Furthermore, RNA-seq data suggest that the ribosome pathway is significantly activated by EAP. It may also link to the cardioprotection in the absence of *Stat5*. In this pathway, we found that Rps6 and Rpl3-ps1 are upregulated by EAP in the *Stat5-cKO* mice. They were reported before to be regulated by the IL-6/STAT3 signaling (Dern *et al.*, 2020; Meyuhas *et al.*, 2015). To confirm this, we determined the mRNA expression in the IL-6/gp130 receptor system, which is an important activator

of STAT3, and have found that the mRNA expressions of gp130 and IL-6 are increased by EAP only in the *Stat5-cKO* mice (Fig 4B), suggesting that when STAT5 is deleted, IL-6/gp130/STAT3 signaling gets activated to play role in the protection against myocardial I/R.

Growing evidence has demonstrated the favorable and protective role of STAT3 in the heart (Harhous *et al*, 2019; Nakao *et al*, 2020). To understand the mechanisms by which STAT3 contributes to protection of EAP against I/R injury, we determined the apoptotic and survival signaling in the heart tissue of the mice. STAT3 is involved in decreasing cardiac I/R injury by reducing apoptosis or increasing anti-apoptotic signaling, increasing expression of cardioprotective proteins, decreasing ROS generation, and inhibiting autophagy (Harhous *et al*, 2019). We found that EAP promoted the expression of anti-apoptotic proteins Bcl-2 and Bcl-xl and p-AKT in the *Stat5^{fl/fl}*+I/R mice, but not in the *Stat5-cKO*+I/R mice. However, the expression of IL-10 protein was increased in both the *Stat5^{fl/fl}* and the *Stat5-cKO* mice when EAP was applied followed by I/R injury. IL-10 is one of the important anti-inflammatory cytokines which can be produced by most cells and affect the growth and differentiation of various hematopoietic cells and increase cell proliferation, angiogenesis, and immune evasion (Zhen *et al*, 2018; Hodge *et al*, 2005). Our previous study has shown that IL-10 RIPC can activate the expression of IL-10, p-AKT, Bcl-2, and Bcl-xl to protect the myocardium (Chen *et al*, 2018). Recently, Takahashi J *et al*. has shown that interleukin-22, one member of the IL-10 cytokine family, activates myocardial STAT3 signaling pathway and prevents myocardial I/R injury in the mouse model of ischemia reperfusion injury (Takahashi *et al*, 2020). Other studies have also shown that the IL-6 and IL-10 family of cytokines are the main mediators that activate intrinsic JAK/STAT3 signaling to induce the transcription of genes enabling survival and proliferation of cells (Harhous *et al*, 2019; Huynh *et al*, 2017). Activated STAT3 can regulate the expression of genes (such as MMP2, MMP9, and Ubc13) and therefore underpin the molecular cross-talk between these genes (Pipicz *et al*, 2018). When the *Stat5-cKO* mice were given a stress of myocardial I/R injury in this study, *Mmp3*, *Ubb*, and *Myh7* genes that are closely correlated with STAT3 pathway were altered by EAP (Table 1b), therefore STAT3 might have played a vital role in cardio-protection by controlling these gene's expression. In addition, some studies have identified that activation of STAT3 can improve the expression VEGF (Huynh *et al*, 2019; Johnson *et al*, 2018). We have

detected the expression of VEGF-A, but there is no difference among our four groups (Appendix Fig 9). To a certain extent, these results show that the activation of STAT3 by EAP may be not enough for elevating angiogenesis in the *Stat5-cKO* mice.

In summary, the present study demonstrates that EAP approach to protecting against myocardial I/R injury by reducing the myocardial infarct area and activating anti-apoptotic and survival signaling. STAT5 is involved in this process but the protection is not STAT5 dependent. STAT3 may compensate the function of STAT5 by activating the IL-6/gp130/STAT3 signaling pathway in the absence of STAT5. This study suggests, for the first time, that EAP can mimic RIPc but function more effectively in cardio-protection against I/R injury through multiple pathways.

Materials and Methods

Antibodies and reagents

Antibodies for p-STAT5 (Try694), p-STAT3 (Try705), STAT3, p-AKT (Ser473), AKT, Cytochrome c (Cyt c), Bcl-xL, Bcl-2, and GAPDH were purchased from Cell Signaling Technology. Antibodies for IL-10, and β -actin were purchased from Abcam (Cambridge, UK). The in-situ cell-death detection kit to assess apoptosis, POD (TUNEL), was purchased from Roche (Lewes, UK). The triphenyltetrazolium chloride (TTC) was purchased from Sigma-Aldrich (St. Louis, MO, USA).

Conditional and inducible cardiomyocyte-specific *Stat5-cKO* mice

As previously described, the *Stat5* mice (*Stat5^{fl/fl}*) were kindly provided by Dr. Hennighausen (NIDDK, NIH), and *Tnnt2-Cre* male mice (*Tnnt2^{Cre}*) were obtained from Bin Zhou (Shanghai Institutes for Biological Sciences of the Chinese Academy of Sciences) as gifts (Chen *et al.*, 2018). The *Stat5* knockout mice (*Stat5-cKO*) were generated by mating these two genotypes. Doxycycline hyclate (Sigma-Aldrich, St. Louis, MO, USA) was administered through adding into the drinking water of mice at a concentration of 2 mg/ml for 7 days. The method used for genotyping has been described in our previous article (Chen *et al.*, 2018).

Study groups

The mice were divided into four groups: *Stat5^{fl/fl}*+I/R, *Stat5^{fl/fl}*+EA+I/R, *Stat5-cKO*+I/R, and *Stat5-cKO*+EA+I/R. *Stat5^{fl/fl}*+I/R and *Stat5-cKO*+I/R groups were subjected to left anterior descending (LAD) coronary artery occlusion for 30min, and then reperfused for 180 min. *Stat5^{fl/fl}*+EA+I/R and *Stat5-cKO*+EA+I/R groups were subjected to EAP 7 days before the LAD ligation. All murine studies were carried out in accordance with the EU Directive 2010/63/EU for the protection of

animals used for experimental purpose. All experiments were approved by the Institute for Animal Care and Use Committee at Nanjing University of Chinese Medicine.

In vivo experiments

Prior to the myocardial I/R injury experiment, *Stat5^{fl/fl}*+EA+I/R and *Stat5-cKO*+EA+I/R mice were pretreated with EA for a total of 7 days. EA was performed at bilateral PC6 (also called Neiguan) acupoints based on the previous study (Huang *et al*, 2014). The PC6 acupoint is located in the interosseal muscles between the radius and ulna of the forelimb, 3 mm proximal to the wrist crease, according to the textbook of experimental acupuncture in animals (Huang *et al*, 2014). Mice were anaesthetized with isoflurane (5%) and maintained with 1-2% isoflurane in pure oxygen. The sterilized disposable stainlesssteel acupuncture needles (0.18mm×13mm, Beijing Zhongyan Taihe Medical Instruments Factory, Beijing, China) were inserted a depth of 1-2mm into the muscle layer at bilateral PC6 simultaneously using Han's EA instrument (Han Acuten, WQ1002F, Beijing, China) and alternating dense and disperse mode, with a frequency of 2/15 Hz at an intensity level of 0.5-1mA, at a stimulation period of 20 minutes, once a day, for a total 7 days. The mice in the *Stat5^{fl/fl}*+I/R group and the *Stat5-cKO*+I/R group were restrained for 20 minutes without EA stimulation.

The I/R operation was performed as described in the previous studies (Chen *et al*, 2018; Huang *et al*, 2014). Briefly, all the mice were given 5% isoflurane and then maintained with 2% isoflurane in a mixture of 70% N₂O and 30% O₂ for anesthesia. Under the anesthetized state, the mice were subjected to a left thoracotomy and LAD ligation with a slipknot using 6-0 silk sutures transiently at 2 to 3 mm below the left auricle, resulting in arterial occlusion, as evidenced by myocardial blanching and electrocardiographic abnormalities (ST-segment elevation and QRS complex widening) (Chen *et al*, 2018). After 30 min, reperfusion was performed by quickly releasing and removing the suture and continued for 3h. In the sham-operation group, the same procedure was performed except for the LAD ligation. Mice were sacrificed after surgery and the heart specimens were harvested.

Determination of infarct size

At the end of the protocol, sections of mouse heart were perfused for 1-2 min with 2ml of 2% TTC (Sigma-Aldrich Co., St. Louis, MO, USA) in phosphate-buffered saline (PBS) and then incubated in an identical solution at 37°C

for 15 min. After incubating, slices were placed in 4% (v/v) paraformaldehyde at 4°C for 12h. TTC stained area (red, normal area) and non-stained areas (white, infarct area) were photographed. The infarcted area was quantified using Image-Pro Plus 6.0 software (NIH, USA). All analyses of infarct size were performed by two investigators who were blinded with the information regarding group assignments.

Apoptosis measurements

TUNEL staining method was used to detect cell apoptosis of cardiac tissue in each group. All the protocols were the same as previously described (Chen *et al*, 2018). Heart tissues were harvested and embedded with OCT (Thermo Scientific™, USA). The 8µm thick tissues were subjected to TUNEL staining according to the manufacturer's instructions for an In-Situ Cell Death Detection Kit (Cat. 11684817910, Roche Diagnostics, Indianapolis, IN, USA). Sections were then visualized with a fluorescence microscope (Nikon, Japan) with parallel positive control (DNase-I) and negative control (label solution only).

Western blotting

Whole ventricle samples were lysed with RIPA buffer supplemented with a protease inhibitor cocktail and a phosphatase inhibitor cocktail (Chen *et al*, 2018). Homogenates were centrifuged at 14,000×g for 10 min at 4 °C, and supernatants were stored at -80 °C until further uses. Protein concentrations were determined using a BCA protein assay (Pierce). Protein was mixed with 5× Laemmli loading buffer and heated at 95 °C for 10 min. Equal amount of protein was subjected to SDS-PAGE and transferred to polyvinylidene fluoride (PVDF) membranes. Immunoblots were performed using appropriate primary antibodies against Bcl-xL (1:1000, Cell Signaling, #2762), Bcl-2 (1:1000, Cell Signaling, #3498), Cyt c (1:1000, Cell Signaling, #6808), Phospho-STAT5 (1:1000, Cell Signaling, #9662), STAT5(1:1000, Cell Signaling, #3421), Phospho-STAT3 (1:1000, Cell Signaling, #2775), STAT3 (1:1000, Cell Signaling, #2612), Phospho-AKT (1:1000, Cell Signaling, #9662), AKT (1:1000, Cell Signaling, #9608), IL-10 (1:1000, Cell Signaling, #4351), β-actin (1:1000, Cell Signaling, #1721), or GAPDH (1:1000, Cell Signaling, #1752) overnight at 4°C, then incubated with a secondary antibody for two hours at room temperature. Western blot band intensities were quantified using SuperSignal West Pico Chemiluminescent substrate (Pierce).

q-PCR analysis

Three micrograms of RNA were converted to cDNA using reverse transcriptase

and random primers (11121ES60, Yeasen Biotech Co., Ltd., China). For PCR analysis, the samples were amplified in duplication using SYBR Green (Vazyme, Q431-02) with 200 nM of gene-specific primers and run on the CFX amplifier (MX3000P, Stratagene, La Jolla, CA, USA) according to the manufacturer's protocol. Data were analyzed by the threshold cycle (Ct) relative-quantification method. The primer sequences were as follow: interleukin-6 (IL-6, forward: GACTTCACAGAG GATACCACCC, reverse: GACTTCACAGAGGATACCACCC); gp130 (forward: GAGCTTCGAGCCATCCGGGC, reverse: AAGTTCGAGCCGCGCTGGAC); Actin (forward: GGTGAAGACGCCAGTAGAC, reverse: TGCTGGAAGGTGGACAGTGA).

RNA-seq and computational analysis for RNA-seq data

To further explore possible changes in transcriptome profile caused by EAP against myocardial I/R injury in the *Stat5* knockout mice, RNA-seq for the mouse heart tissues were performed using next generation high throughput sequencing method (Illumina HiSeq 2000, Illumina). Total RNAs were isolated. The RNA-seq protocol was described in our previous study (Fu *et al*, 2017).

Data analysis was performed as previously described (Fu *et al*, 2017). Quality of raw sequencing data was assessed by FASTQ files. We used the Cufflinks program and the Cuffdiff program to assemble individual transcripts and differential transcript expression analysis. The pathways were analyzed using the DAVID Bioinformatics Resources. Genes with lower than 1.0 FPKM (average fragments per kilobase of transcript per million fragments mapped) filtered out. Up-regulated and down-regulated genes were defined as a relative transcription level of above Log₂ fold change (FC) $\geq |\pm 1|$ and *P* value <0.05.

The paper explained

Problem

Our recent study has shown that signal transducer and activator of transcription 5 (STAT5) plays a critical role in RIPC, and RIPC mediates cardioprotection by activating anti-apoptotic and cardiomyocyte-survival signaling in a STAT5-dependent manner (Chen *et al*, 2018). Studies, including our previous work, have shown that using electro-acupuncture before the event of ischemia-reperfusion, which is also called electro-acupuncture pretreatment (EAP), could protect cardiomyocytes by reducing the myocardial infarct size and regulating some molecular signaling (Huang *et al*, 2014; Lu *et al*, 2016). Given that the main molecule involved in RIPC in human patients is STAT5 (Cheung *et al*, 2006; Chen *et al*, 2018), we question whether EAP shares the same mechanism with RIPC and plays a preconditioning-like role as RIPC does on I/R injury.

Result

The present study demonstrates that EAP can protect against myocardial I/R injury by reducing the myocardial infarct area and activating anti-apoptotic and survival signaling. STAT5 is involved in this process but the protection is not STAT5 dependent. STAT3 may compensate the function of STAT5 by activating the IL-6/gp130/STAT3 signaling pathway in the absence of STAT5. We revealed, for the first time, that EAP can mimic RIPC but function more effectively in cardio-protection against I/R injury through multiple pathways.

Impact

This study will provide new scientific experimental data for acupuncture protecting against I/R injury.

Statistics

SPSS18.0 statistical software was utilized for statistical analysis. All data were presented as the mean \pm standard error of mean (SEM). The significance of the differences was determined by Student's t-test or one-way analysis of variance (ANOVA) with the least significant difference post hoc test when equal variances were assumed or with Bonferroni test post hoc when equal variances were not assumed. $P < 0.05$ was considered statistically significant.

Data availability

The data supporting this study is available from the corresponding author upon reasonable request. RNA-Seq raw data is available in the National Center for Biotechnology Information

(NCBI) Gene Expression Omnibus (GEO) with the accession number GSExxxxx

(<https://www.ncbi.nlm.nih.gov/geo/query/acc.cgi?acc=GSExxxxx>).

Expanded View for this article is available online

Acknowledgements

This research was supported by the National Key R&D Program of China (No. 2019YFC1709003), the National Natural Science Foundation of China (Grant No. 81870224). We thank Dr. Wanxin Liu (Washington DC, USA) for language editing.

Author contribution

Bing-mei Zhu and Xin-yue Jing conceived and supervised experiments. Hui-hui Guo, Xin-yue Jing, Hui Chen and Bing-mei Zhu wrote and edited the manuscript. Hui Chen and Hui-hui Guo performed experiments and analyzed data. Hou-xi Xu carried out the bioinformatic analyses for RNA-seq.

Conflict of interest

The authors declare that they have no conflict of interest.

supplementary material.

manuscriptID_Figure 9.

References

- Abilleira S, Bevan S, Markus HS (2006) The role of genetic variants of matrix metalloproteinases in coronary and carotid atherosclerosis. *J Med Genet* 43(12):897-901.
- Alam MJ, Gupta R, Mahapatra NR, Goswami SK (2020) Catestatin reverses the hypertrophic effects of norepinephrine in H9c2 cardiac myoblasts by modulating the adrenergic signaling. *Mol Cell Biochem* 464(1-2):205-219.
- Alfonso-Jaume MA, Bergman MR, Mahimkar R, Cheng S, Jin ZQ, Karliner JS, Lovett DH (2006) Cardiac ischemia-reperfusion injury induces matrix metalloproteinase-2 expression through the AP-1 components FosB and JunB. *Am J Physiol Heart Circ Physiol* 291(4):H1838-46.
- Abilleira S, Bevan S, Markus HS (2006) The role of genetic variants of matrix metalloproteinases in coronary and carotid atherosclerosis. *J Med Genet* 43(12):897-901.
- Bos JM, Subramaniam M, Hawse JR, Christiaans I, Rajamannan NM, Maleszewski JJ, Edwards WD, Wilde AA, Spelsberg TC, Ackerman MJ (2012) TGF β -inducible early gene-1 (TIEG1) mutations in hypertrophic cardiomyopathy. *J Cell Biochem* 113(6):1896-903.
- Binder A, Ali A, Chawla R, Aziz HA, Abbate A, Jovin IS (2015) Myocardial protection from ischemia-reperfusion injury post coronary revascularization. *Expert Rev Cardiovasc Ther.* 13(9):1045-57.
- Chen J, Luo Y, Wang S, Zhu H, Li D (2019) Roles and mechanisms of SUMOylation on key proteins in myocardial ischemia/reperfusion injury. *J Mol Cell Cardiol* 134:154-164.
- Cho YJ, Kim WH (2019) Perioperative Cardioprotection by Remote Ischemic Conditioning. *Int J Mol Sci* 20(19). pii: E4839.
- Chen H, Jing XY, Shen YJ, Wang TL, Ou C, Lu SF, Cai Y, Li Q, Chen X, Ding YJ, Yu XC, Zhu BM (2018) Stat5-dependent Cardioprotection in Late Remote Ischemia Preconditioning. *Cardiovasc Res* 114(5):679-689.
- Cheung MM, Kharbanda RK, Konstantinov IE, Shimizu M, Frndova H, Li J, Holtby HM, Cox PN, Smallhorn JF, Van Arsdell GS, Redington AN (2006) Randomized controlled trial of the effects of remote ischemic preconditioning on children undergoing cardiac surgery: first clinical application in humans. *J Am Coll Cardiol* 47(11):2277-82.
- Castejon ML, Sánchez-Hidalgo M, Aparicio-Soto M, Montoya T, Martín-LaCave I, Fernández-Bolaños JG, Alarcón-de-la-Lastra C (2019) Dietary oleuropein and its new acyl-derivate attenuate murine lupus nephritis through HO-1/Nrf2 activation and suppressing JAK/STAT, NF- κ B, MAPK and NLRP3 inflammasome signaling pathways. *J Nutr Biochem*

74:108229.

Calamaras TD, Lee C, Lan F, Ido Y, Siwik DA, Colucci WS (2015) The lipid peroxidation product 4-hydroxy-trans-2-nonenal causes protein synthesis in cardiac myocytes via activated mTORC1-p70S6K-RPS6 signaling. *Free Radic Biol Med* 82:137-46.

Cai Y, Ying F, Liu H, Ge L, Song E, Wang L, Zhang D, Hoi Ching Tang E, Xia Z, Irwin MG (2020) Deletion of Rap1 protects against myocardial ischemia/reperfusion injury through suppressing cell apoptosis via activation of STAT3 signaling. *FASEB J* doi: 10.1096/fj.201901592RR.

Cao CM, Zhang Y, Weisleder N, Ferrante C, Wang X, Lv F, Zhang Y, Song R, Hwang M, Jin L, Guo J, Peng W, Li G, Nishi M, Takeshima H, Ma J, Xiao RP (2010) MG53 constitutes a primary determinant of cardiac ischemic preconditioning. *Circulation* 121(23):2565-74.

Calamaras TD, Lee C, Lan F, Ido Y, Siwik DA, Colucci WS (2015) The lipid peroxidation product 4-hydroxy-trans-2-nonenal causes protein synthesis in cardiac myocytes via activated mTORC1-p70S6K-RPS6 signaling. *Free Radic Biol Med* 82:137-46.

Chen H, Shao X, Li L, Zheng C, Xu X, Hong X, Li X, Wu M (2017) Electroacupuncture serum inhibits TNF- α -mediated chondrocyte inflammation via the Ras-Raf-MEK1/2-ERK1/2 signaling pathway. *Mol Med Rep* 16(5):5807-5814.

Chen Q, Jin M, Yang F, Zhu J, Xiao Q, Zhang L (2013) Matrix metalloproteinases: inflammatory regulators of cell behaviors in vascular formation and remodeling. *Mediators Inflamm* 2013:928315.

Davidson SM, Ferdinandy P, Andreadou I, Bøtker HE, Heusch G, Ibáñez B, Ovize M, Schulz R, Yellon DM, Hausenloy DJ, Garcia-Dorado D (2019) Multitarget Strategies to Reduce Myocardial Ischemia/Reperfusion Injury: JACC Review Topic of the Week. *J Am Coll Cardiol* 73(1):89-99.

Dern K, Burns TA, Watts MR, van Eps AW, Belknap JK (2019) Influence of digital hypothermia on lamellar events related to IL-6/gp130 signalling in equine sepsis-related laminitis. *Equine Vet J* doi: 10.1111/evj.13184.

Dai QF, Gao JH, Xin JJ, *et al* (2019) The Role of Adenosine A2b Receptor in Mediating the Cardioprotection of Electroacupuncture Pretreatment via Influencing Ca²⁺ Key Regulators. *Evid Based Complement Alternat Med* 6721286.

Dern K, Burns TA, Watts MR, van Eps AW, Belknap JK (2019) Influence of digital hypothermia on lamellar events related to IL-6/gp130 signalling in equine sepsis-related laminitis. *Equine Vet J* doi: 10.1111/evj.13184.

Dern K, Burns TA, Watts MR, van Eps AW, Belknap JK (2020) Influence of digital hypothermia on lamellar events related to IL-6/gp130 signalling in equine sepsis-related

laminitis. *Equine Vet. J* 52(3).

Ekeloef S, Homilius M, Stilling M, Ekeloef P, Koyuncu S, Münster AB, Meyhoff CS, Gundel O, Holst-Knudsen J, Mathiesen O, Gögenur I (2019) The effect of remote ischaemic preconditioning on myocardial injury in emergency hip fracture surgery (PIXIE trial): phase II randomised clinical trial. *BMJ* 367:l6395.

El-Magd MA, Abdo WS, El-Maddaway M, Nasr NM, Gaber RA, El-Shetry ES, Saleh AA, Alzahrani FAA, Abdelhady DH (2017) High doses of S-methylcysteine cause hypoxia-induced cardiomyocyte apoptosis accompanied by engulfment of mitochondria by nucleus. *Biomed Pharmacother* 94:589-597.

Ekeloef S, Homilius M, Stilling M, Ekeloef P, Koyuncu S, Münster AB, Meyhoff CS, Gundel O, Holst-Knudsen J, Mathiesen O, Gögenur I (2019) The effect of remote ischaemic preconditioning on myocardial injury in emergency hip fracture surgery (PIXIE trial): phase II randomised clinical trial. *BMJ* 367:l6395.

Fu SP, He SY, Xu B, Hu CJ, Lu SF, Shen WX, Huang Y, Hong H, Li Q, Wang N, Liu XL, Liang F, Zhu BM (2014) Acupuncture promotes angiogenesis after myocardial ischemia through H3K9 acetylation regulation at VEGF gene. *PLoS One* 9(4):e94604.

Fu SP, Hong H, Lu SF, Hu CJ, Xu HX, Li Q, Yu ML, Ou C, Meng JZ, Wang TL, Hennighausen L, Zhu BM (2017) Genome-wide regulation of electro-acupuncture on the neural Stat5-loss-induced obese mice. *PLoS One* 12(8):e0181948.

Friedbichler K, Themanns M, Mueller KM, Schleder M, Kornfeld JW, Terracciano LM, Kozlov AV, Haindl S, Kenner L, Kolbe T, Mueller M, Snibson KJ, Heim MH, Moriggl R (2012) Growth-hormone-induced signal transducer and activator of transcription 5 signaling causes gigantism, inflammation, and premature death but protects mice from aggressive liver cancer. *Hepatology* 55(3):941-52.

Geng Y, Chen D, Zhou J, Lu J, Chen M, Zhang H, Wang X (2016) Synergistic Effects of Electroacupuncture and Mesenchymal Stem Cells on Intestinal Ischemia/Reperfusion Injury in Rats. *Inflammation* 39(4):1414-20.

Heusch G (2015) Molecular basis of cardioprotection: signal transduction in ischemic pre-, post-, and remote conditioning. *Circ Res* 116(4):674-99.

Huang Y, Lu SF, Hu CJ, Fu SP, Shen WX, Liu WX, Li Q, Wang N, He SY, Liang FR, Zhu BM (2014) Electro-acupuncture at Neiguan pretreatment alters genome-wide gene expressions and protects rat myocardium against ischemia-reperfusion. *Molecules* 19(10):16158-78.

Huang S, Liu Q, Liao Q, Wu Q, Sun B, Yang Z, Hu X, Tan M, Li L (2018) Interleukin-6/signal transducer and activator of transcription 3 promotes prostate cancer resistance to androgen

- deprivation therapy via regulating pituitary tumor transforming gene 1 expression. *Cancer Sci* 109(3):678-687.
- Hausenloy DJ, Kharbanda RK, Møller UK, *et al* (2019) Effect of remote ischaemic conditioning on clinical outcomes in patients with acute myocardial infarction (CONDI-2/ERIC-PPCI): a single-blind randomised controlled trial. *Lancet* 394(10207):1415-1424.
- Huang S, Liu Q, Liao Q, Wu Q, Sun B, Yang Z, Hu X, Tan M, Li L (2018) Interleukin-6/signal transducer and activator of transcription 3 promotes prostate cancer resistance to androgen deprivation therapy via regulating pituitary tumor transforming gene 1 expression. *Cancer Sci*. 109(3):678-687.
- Hennighausen L, Robinson GW (2008) Interpretation of cytokine signaling through the transcription factors STAT5A and STAT5B. *Genes Dev* 22(6):711-21.
- Hosui A, Kimura A, Yamaji D, Zhu BM, Na R, Hennighausen L(2009) Loss of STAT5 causes liver fibrosis and cancer development through increased TGF- β and STAT3 activation. *J Exp Med* 206(4):819-31.
- Hin Tang JJ, Hao Thng DK, Lim JJ, Toh TB (2020) JAK/STAT signaling in hepatocellular carcinoma. *Hepat Oncol* 7(1):HEP18.
- Harhous Z, Booz GW, Ovize M, Bidaux G, Kurdi M (2019) An Update on the Multifaceted Roles of STAT3 in the Heart. *Front Cardiovasc Med* 6:150.
- Hodge DR, Hurt EM, Farrar WL (2005) The role of IL-6 and STAT3 in inflammation and cancer. *Eur J Cancer* 41(16):2502-12.
- Huynh J, Etemadi N, Hollande F, Ernst M, Buchert M (2017)The JAK/STAT3 axis: A comprehensive drug target for solid malignancies. *Semin Cancer Biol* 45:13-22.
- Huynh J, Chand A, Gough D, Ernst M (2019) Therapeutically exploiting STAT3 activity in cancer - using tissue repair as a road map. *Nat. Rev. Cancer* 19(2).
- Haque I, Ghosh A, Acup S, Banerjee S, Dhar K, Ray A, Sarkar S, Kambhampati S, Banerjee SK (2018), Leptin-induced ER- α -positive breast cancer cell viability and migration is mediated by suppressing CCN5-signaling via activating JAK/AKT/STAT-pathway. *BMC Cancer* 18(1).
- Yuan N, Yu G, Liu D, Wang X, Zhao L(2019). An emerging role of interleukin-23 in rheumatoid arthritis. *Immunopharmacol Immunotoxicol* 41(2):185-191.
- Yellon DM, Hausenloy DJ (2017). Myocardial reperfusion injury. *N Engl J Med* 357(11):1121-35.
- Yu JH, Zhu BM, Wickre M, Riedlinger G, Chen W, Hosui A, Robinson GW, Hennighausen L (2010) The transcription factors signal transducer and activator of transcription 5A (STAT5A) and STAT5B negatively regulate cell proliferation through the activation of cyclin-dependent

- kinase inhibitor 2b (Cdkn2b) and Cdkn1a expression. *Hepatology* 52(5):1808-18.
- Ji C, Song F, Huang G, Wang S, Liu H, Liu S, Huang L, Liu S, Zhao J, Lu TJ, Xu F (2018) The protective effects of acupoint gel embedding on rats with myocardial ischemia-reperfusion injury. *Life Sci* 211:51-62.
- Jiang Y, Feng YP, Tang LX, Yan YL, Bai JW (2019) The protective role of NR4A3 in acute myocardial infarction by suppressing inflammatory responses via JAK2-STAT3/NF- κ B pathway. *Biochem Biophys Res Commun* 517(4):697-702.
- Janson ND, Jehanathan N, Jung S, Priyathilaka TT, Nam BH, Kim MJ, Lee J (2019) Insight into the molecular function and transcriptional regulation of activator protein 1 (AP-1) components c-Jun/c-Fos ortholog in red lip mullet (*Liza haematocheila*). *Fish Shellfish Immunol* 93:597-611.
- Ji Z, Liang J, Wu J, Zhang Y, Jia W (2019) Effects of electroacupuncture at Taichong (LR 3) and Baihui (DU 20) on cardiac hypertrophy in rats with spontaneous hypertension. *J Tradit Chin Med* 39(4):502-508.
- Jiang B, Liang P, Wang K, Lv C, Sun L, Tong Z, Liu Y, Xiao X (2014) Nucleolin involved in myocardial ischaemic preconditioning via post-transcriptional control of HSPA1A expression. *Cardiovasc. Res* 102(1).
- Johnson DE, O'Keefe RA, Grandis JR (2018) Targeting the IL-6/JAK/STAT3 signalling axis in cancer. *Nat Rev Clin Oncol* 15(4).
- Kubota A, Suto A, Suzuki K, Kobayashi Y, Nakajima H (2019) Matrix metalloproteinase-12 produced by Ly6C macrophages prolongs the survival after myocardial infarction by preventing neutrophil influx. *J. Mol. Cell. Cardiol* 131.
- Kim HJ, Park HJ, Hong MS, Song JY, Park HK, Jo DJ, Park SW, HwanYun D, Park HK, Yang JS, Ban JY, Chung JH (2010) Effect by acupuncture on hypothalamic expression of maternally separated rats: proteomic approach. *Neurol Res* 32 Suppl 1:69-73.
- Li Y, Chen B, Yang X, Zhang C, Jiao Y, Li P, Liu Y, Li Z, Qiao B, Bond Lau W, Ma XL, Du J (2019) S100a8/a9 Signaling Causes Mitochondrial Dysfunction and Cardiomyocyte Death in Response to Ischemic/Reperfusion Injury. *Circulation* 140(9):751-764.
- Lu SF, Huang Y, Wang N, Shen WX, Fu SP, Li Q, Yu ML, Liu WX, Chen X, Jing XY, Zhu BM (2016) Cardioprotective Effect of Electroacupuncture Pretreatment on Myocardial Ischemia / Reperfusion Injury via Antiapoptotic Signaling. *Evid Based Complement Alternat Med* 1-9.
- Lai YJ, Tsai JC, Tseng YT, Wu MS, Liu WS, Lam HI, Yu JH, Nozell SE, Benveniste EN (2017) Small G protein Rac GTPases regulate the maintenance of glioblastoma stem-like cells in vitro and in vivo. *Oncotarget* 8(11):18031-18049.

- Lai YJ, Tsai JC, Tseng YT, Wu MS, Liu WS, Lam HI, Yu JH, Nozell SE, Benveniste EN (2017) Small G protein Rac GTPases regulate the maintenance of glioblastoma stem-like cells in vitro and in vivo. *Oncotarget* 8(11):18031-18049.
- Lindsey ML(2018) Assigning matrix metalloproteinase roles in ischaemic cardiac remodelling. *Nat Rev Cardiol* 15(8):471-479.
- Ma P, Li Y, Wang S, Wang G, Yan C, Li Z, Wang Y, Qin F, Chen L, Fu P (2020) SOCS3 promotes myocardial cell apoptosis in myocardial ischemia reperfusion rats via JAK/STAT signaling pathway. *Minerva Cardioangiol*.
- Meyuhas O (2015) Ribosomal Protein S6 Phosphorylation: Four Decades of Research. *Int Rev Cell Mol Biol* 320.
- Nakao S, Tsukamoto T, Ueyama T, Kawamura T (2020) STAT3 for Cardiac Regenerative Medicine: Involvement in Stem Cell Biology, Pathophysiology, and Bioengineering. *Int J Mol Sci* 21(6). pii: E1937.
- Oba T, Yasukawa H, Hoshijima M, Sasaki K, Futamata N, Fukui D, Mawatari K, Nagata T, Kyogoku S, Ohshima H, Minami T, Nakamura K, Kang D, Yajima T, Knowlton KU, Imaizumi T (2012) Cardiac-specific deletion of SOCS-3 prevents development of left ventricular remodeling after acute myocardial infarction. *J Am Coll Cardiol* 59(9):838-52.
- Obana M, Maeda M, Takeda K, Hayama A, Mohri T, Yamashita T, Nakaoka Y, Komuro I, Takeda K, Matsumiya G, Azuma J, Fujio Y (2010) Therapeutic activation of signal transducer and activator of transcription 3 by interleukin-11 ameliorates cardiac fibrosis after myocardial infarction. *Circulation* 121(5):684-91.
- Painovich J, Longhurst J (2015) Integrating acupuncture into the cardiology clinic: can it play a role? *Sheng Li Xue Bao* 67(1):19-31.
- Pipicz M, Demján V, Sárközy M, Csont T(2018) Effects of Cardiovascular Risk Factors on Cardiac STAT3. *Int J Mol Sci* 19(11). pii: E3572.
- Świerkot J, Sokolik R, Czarny A, Zaczyńska E, Nowak B, Chlebicki A, Korman L, Madej M, Wojtala P, Lubiński Ł, Wiland P (2015) Activity of JAK/STAT and NF-κB in patients with axial spondyloarthritis. *Postepy Hig Med Dosw (Online)* 69:1291-8.
- Sun S, Cui Z, Yan T, Wu J Liu Z (2019) CCN5 inhibits proliferation and promotes apoptosis of oral squamous cell carcinoma cells. *Cell Biol Int* doi: 10.1002/cbin.11296.
- Stobdan T, Zhou D, Ao-Ieong E, Ortiz D, Ronen R, Hartley I, Gan Z, McCulloch AD, Bafna V, Cabrales P, Haddad GG (2015) Endothelin receptor B, a candidate gene from human studies at high altitude, improves cardiac tolerance to hypoxia in genetically engineered heterozygote mice. *Proc Natl Acad Sci U S A* 112(33):10425-30.

- Sharma S, Mazumder AG, Rana AK, Patial V, Singh D (2019) Spontaneous Recurrent Seizures Mediated Cardiac Dysfunction via mTOR Pathway Upregulation: A Putative Target for SUDEP Management. *CNS Neurol Disord Drug Targets* 18(7):555-565.
- Sulston R, Kelly V, Walker BR, Porter KE, Chapman KE, Gray GA (2017) 11 β -HSD1 suppresses cardiac fibroblast CXCL2, CXCL5 and neutrophil recruitment to the heart post MI. *J Endocrinol* 233(3):315-327.
- Saddic LA, Howard-Quijano K, Kipke J, Kubo Y, Dale EA, Hoover D, Shivkumar K, Eghbali M, Mahajan A (2018) Progression of myocardial ischemia leads to unique changes in immediate-early gene expression in the spinal cord dorsal horn. *Am J Physiol Heart Circ Physiol* 315(6):H1592-H1601.
- Shirakawa K, Endo J, Kataoka M, Katsumata Y, Yoshida N, Yamamoto T, Isobe S, Moriyama H, Goto S, Kitakata H, Hiraide T, Fukuda K, Sano M (2018) IL (Interleukin)-10-STAT3-Galectin-3 Axis Is Essential for Osteopontin-Producing Reparative Macrophage Polarization After Myocardial Infarction. *Circulation* 138(18):2021-2035.
- Shirakawa K, Endo J, Kataoka M, Katsumata Y, Yoshida N, Yamamoto T, Isobe S, Moriyama H, Goto S, Kitakata H, Hiraide T, Fukuda K, Sano M (2018) IL (Interleukin)-10-STAT3-Galectin-3 Axis Is Essential for Osteopontin-Producing Reparative Macrophage Polarization After Myocardial Infarction. *Circulation* 138(18):2021-2035.
- Gupta R, Wood DA (2019) Primary prevention of ischaemic heart disease: populations, individuals, and health professionals. *Lancet*. 394(10199):685-696.
- Gopinath SD (2017) Inhibition of Stat3 signaling ameliorates atrophy of the soleus muscles in mice lacking the vitamin D receptor. *Skelet Muscle* 7(1):2.
- Sharma S, Mazumder AG, Rana AK, Patial V, Singh D (2019) Spontaneous Recurrent Seizures Mediated Cardiac Dysfunction via mTOR Pathway Upregulation: A Putative Target for SUDEP Management. *CNS Neurol Disord Drug Targets* 18(7):555-565.
- Shirakawa K, Endo J, Kataoka M, Katsumata Y, Yoshida N, Yamamoto T, Isobe S, Moriyama H, Goto S, Kitakata H, Hiraide T, Fukuda K, Sano M (2018) IL (Interleukin)-10-STAT3-Galectin-3 Axis Is Essential for Osteopontin-Producing Reparative Macrophage Polarization After Myocardial Infarction. *Circulation* 138(18):2021-2035.
- Tian X, Wang Y, Li S, Yue W, Tian H (2020) ZHX2 inhibits proliferation and promotes apoptosis of human lung cancer cells through targeting p38MAPK pathway. *Cancer Biomark* 27(1):75-84.
- Takahashi J, Yamamoto M, Yasukawa H, Nohara S, Nagata T, Shimozone K, Yanai T, Sasaki T, Okabe K, Shibata T, Mawatari K, Kakuma T, Aoki H, Fukumoto Y (2020) Interleukin-22 Directly Activates Myocardial STAT3 (Signal Transducer and Activator of Transcription-3)

- Signaling Pathway and Prevents Myocardial Ischemia Reperfusion Injury. *J Am Heart Assoc* 9(8):e014814.
- Tang Y, Wang Y, Park KM, Hu Q, Teoh JP, Broskova Z, Ranganathan P, Jayakumar C, Li J, Su H, Tang Y, Ramesh G, Kim IM (2019) MicroRNA-150 protects the mouse heart from ischaemic injury by regulating cell death. *J Mol Cell Cardiol* 131:41-52.
- Tang Q, Zhang SQ, Zheng TT, Li JS, Yin X, Qin P, Li HY (2019) The mechanism of electroacupuncture preconditioning improved myocardial ischemia/reperfusion injury. *World journal of integrated Chinese and western medicine* 3(14):441-443.
- Udoko AN, Johnson CA, Dykan A, Rachakonda G, Villalta F, Mandape SN, Lima MF, Pratap S, Nde PN (2016) Early Regulation of Profibrotic Genes in Primary Human Cardiac Myocytes by *Trypanosoma cruzi*. *PLoS Negl Trop Dis* 10(1):e0003747.
- Valle-Mendiola A, Soto-Cruz I (2020) Energy Metabolism in Cancer: The Roles of STAT3 and STAT5 in the Regulation of Metabolism-Related Genes. *Cancers (Basel)* 12(1). pii: E124.
- Wu JB, Zhou Y, Liang CL, Zhang XJ, Lai JM, Ye SF, Ouyang H, Lin J, Zhou JY (2017) Cyclovirobuxinum D alleviates cardiac hypertrophy in hyperthyroid rats by preventing apoptosis of cardiac cells and inhibiting the p38 mitogen-activated protein kinase signaling pathway. *Chin J Integr Med* 23(10).
- Wang XT, Wu XD, Lu YX, Sun YH, Zhu HH, Liang JB, He WK, Li L (2018) Egr-1 is involved in coronary microembolization-induced myocardial injury via Bim/Beclin-1 pathway-mediated autophagy inhibition and apoptosis activation. *Aging (Albany NY)* 10(11):3136-3147.
- Wu RM, Jiang B, Li H, Dang WZ, Bao WL, Li HD, Ye G, Shen X (2020) A network pharmacology approach to discover action mechanisms of Yangxinshi Tablet for improving energy metabolism in chronic ischemic heart failure. *J Ethnopharmacol* 246:112227.
- Wen Y, Feng D, Wu H, Liu W, Li H, Wang F, Xia Q, Gao WQ, Kong X (2015) Defective Initiation of Liver Regeneration in Osteopontin-Deficient Mice after Partial Hepatectomy due to Insufficient Activation of IL-6/Stat3 Pathway. *Int J Biol Sci* 11(10):1236-47.
- Wang K, Ju Z, Chen C, Fan S, Pei L, Feng C, Wang F, Cui H, Zhou J (2020) Cardioprotective effect of electroacupuncture in cardiopulmonary bypass through apelin/APJ signaling. *Life Sci*. 242:117208.
- Wingelhofer B, Neubauer HA, Valent P, Han X, Constantinescu SN, Gunning PT, Müller M, Moriggl R (2018). Implications of STAT3 and STAT5 signaling on gene regulation and chromatin remodeling in hematopoietic cancer. *Leukemia* 32(8):1713-1726.
- Walker SR, Xiang M, Frank DA (2014) Distinct roles of STAT3 and STAT5 in the pathogenesis and targeted therapy of breast cancer. *Mol Cell Endocrinol* 382(1):616-621.

- Walker SR, Nelson EA, Yeh JE, Pinello L, Yuan GC, Frank DA (2013) STAT5 outcompetes STAT3 to regulate the expression of the oncogenic transcriptional modulator BCL6. *Mol Cell Biol*. 33(15):2879-90.
- Walker SR, Xiang M, Frank DA (2014) STAT3 Activity and Function in Cancer: Modulation by STAT5 and miR-146b. *Cancers (Basel)* 6(2):958-68.
- Wen Z, Liu Q, Wu J, Xu B, Wang J, Liang L, Guo Y, Peng M, Zhao Y, Liao Q (2019) Fibroblast activation protein α -positive pancreatic stellate cells promote the migration and invasion of pancreatic cancer by CXCL1-mediated Akt phosphorylation. *Ann Transl Med* 7(20):532.
- Wen Y, Feng D, Wu H, Liu W, Li H, Wang F, Xia Q, Gao WQ, Kong X (2015) Defective Initiation of Liver Regeneration in Osteopontin-Deficient Mice after Partial Hepatectomy due to Insufficient Activation of IL-6/Stat3 Pathway. *Int J Biol Sci* 11(10):1236-47.
- Wu RM, Jiang B, Li H, Dang WZ, Bao WL, Li HD, Ye G, Shen X (2020) A network pharmacology approach to discover action mechanisms of Yangxinshi Tablet for improving energy metabolism in chronic ischemic heart failure. *J Ethnopharmacol* 246:112227.
- Wingelhofer B, Neubauer HA, Valent P, Han X, Constantinescu SN, Gunning PT, Müller M, Moriggl R (2018) Implications of STAT3 and STAT5 signaling on gene regulation and chromatin remodeling in hematopoietic cancer. *Leukemia* 32(8):1713-1726.
- Walker SR, Xiang M, Frank DA (2014) Distinct roles of STAT3 and STAT5 in the pathogenesis and targeted therapy of breast cancer. *Mol Cell Endocrinol* 382(1):616-621.
- Walker SR, Nelson EA, Yeh JE, Pinello L, Yuan GC, Frank DA (2013) STAT5 outcompetes STAT3 to regulate the expression of the oncogenic transcriptional modulator BCL6. *Mol Cell Biol* 33(15):2879-90.
- Wilhide ME, Tranter M, Ren X, Chen J, Sartor MA, Medvedovic M, Jones WK (2011) Identification of a NF- κ B cardioprotective gene program: NF- κ B regulation of Hsp70.1 contributes to cardioprotection after permanent coronary occlusion. *J. Mol. Cell. Cardiol* 51(1).
- Zhang T, Yang WX, Wang YL, Yuan J, Qian Y, Sun QM, Yu ML, Fu SP, Xu B, Lu SF (2020) Electroacupuncture preconditioning attenuates acute myocardial ischemia injury through inhibiting NLRP3 inflammasome activation in mice. *Life Sci* 248:117451.
- Zeng Q, He H, Wang XB, Zhou YQ, Lin HX, Tan ZP, He SF, Huang GZ (2018) Electroacupuncture Preconditioning Improves Myocardial Infarction Injury via Enhancing AMPK-Dependent Autophagy in Rats. *Biomed Res Int* 2018:1238175.
- Zhai CG, Xu YY, Tie YY, Zhang Y, Chen WQ, Ji XP, Mao Y, Qiao L, Cheng J, Xu QB, Zhang C (2018) DKK3 overexpression attenuates cardiac hypertrophy and fibrosis in an angiotensin-perfused animal model by regulating the ADAM17/ACE2 and GSK-3 β / β -catenin

pathways. *J Mol Cell Cardiol* 114:243-252.

Zhu XM, Sun WF (2017) Association between matrix metalloproteinases polymorphisms and ovarian cancer risk: A meta-analysis and systematic review. *PLoS One* 12(9):e0185456.

Zhang T, Yang WX, Wang YL, *et al* (2020) Electroacupuncture preconditioning attenuates acute myocardial ischemia injury through inhibiting NLRP3 inflammasome activation in mice. *Life Sci.* 248:117451.

Zhao L, Li D, Zheng H, *et al* (2019) Acupuncture as Adjunctive Therapy for Chronic Stable Angina: A Randomized Clinical Trial[J]. *JAMA Intern Med* doi: 10.1001/jamainternmed.

Zhou X, Xia N, Lv B, Tang T, Nie S, Zhang M, Jiao J, Liu J, Xu C, Hou G, Yang X, Hu Y, Liao Y, Cheng X (2020) Interleukin 35 ameliorates myocardial ischemia-reperfusion injury by activating the gp130-STAT3 axis. *FASEB J* doi: 10.1096/fj.201901718RR.

Zhen Z, Li Y, Jinhua Y, Zhen KW, and Gang D (2018) PI3K/Akt and HIF-1 signaling pathway in hypoxia-ischemia. Published online.

Table 1. The top 30 differentially expressed genes with a log₂ (FC) > |±1| and q value < 0.05

A. The top 30 differentially expressed genes obtained from comparing *Stat5^{fl/fl}*+EA+I/R vs *Stat5^{fl/fl}*+I/R

Up-regulated in EA against I/R				down-regulated in EA against I/R			
Gene name	value_1	value_2	log ₂ (fold_change)	Gene name	value_1	value_2	log ₂ (fold_change)
Fosb	0.181422	27.5826	7.24827	Hbb-bt	35.5975	1.35656	-4.71375
Retnlg	1.26857	106.281	6.38853	Tcf15	53.5841	3.7788	-3.82581
Crisp1	1.13838	82.4984	6.17931	Ccn5	6.67781	0.624545	-3.4185
Fos	1.59922	114.642	6.16363	Myl4	60.998	5.99943	-3.34586
Cxcl5	0.375871	21.1825	5.81649	Scand1	105.37	11.7828	-3.16071
Selp	0.314312	16.2764	5.69443	Zhx2	1.93407	0.220615	-3.13204
Cxcl1	1.96399	95.2442	5.59977	Nrtn	43.6184	5.0225	-3.11846
S100a8	5.82634	256.694	5.46131	Tnfrsf25	3.90054	0.503182	-2.95452
Atf3	2.46681	106.299	5.42933	Pttg1	33.8997	4.94227	-2.77803
Ptx3	0.51755	19.8976	5.26476	Zfp771	19.5158	3.02169	-2.69122
Nr4a3	0.472838	17.3526	5.19767	Fzd2	3.1422	0.491571	-2.6763
Sele	0.190666	6.83815	5.16449	Fxyd3	3.78128	0.621019	-2.60617
Socs3	2.33823	83.0272	5.1501	Aplnr	15.2807	2.89142	-2.40186
Egr1	3.52759	122.674	5.12	Cited4	17.5033	3.57884	-2.29006
S100a9	11.0427	381.325	5.10986	Eva1b	18.5641	3.80599	-2.28617
Il18rap	0.0722091	2.21294	4.93764	Msx1	3.34857	0.6924	-2.27387
Thbs1	1.59068	41.5123	4.70582	Dkk3	5.70321	1.21389	-2.23213
Rdh12	0.122831	3.01114	4.61557	Rnaset2a	22.5668	4.88218	-2.2086
Hspa1b	2.40171	58.418	4.60428	Ifi2712a	180.402	39.5256	-2.19036
Hspa1a	1.99294	44.6613	4.48606	Nrarp	11.2641	2.52363	-2.15815
Adam8	0.400678	8.43168	4.39531	Kctd15	2.65098	0.611701	-2.11563
Ch25h	0.769351	15.8707	4.36658	Hic1	7.47804	1.74196	-2.10195
Nts	0.799365	15.3258	4.26096	Gas1	16.0842	3.82293	-2.07289
Ifitm6	1.20354	22.6423	4.23367	Oas1a	3.5286	0.843947	-2.06387
Egr2	0.16011	3.01005	4.23265	Dynll1	78.6361	18.9174	-2.05548

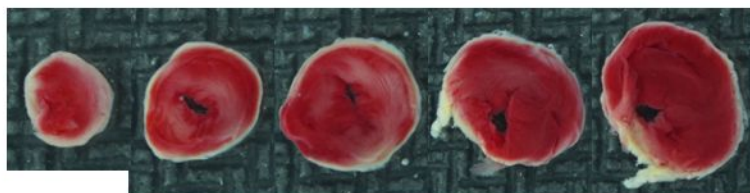
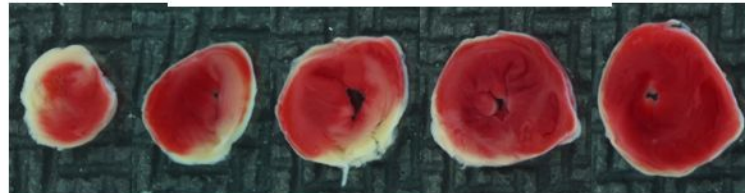
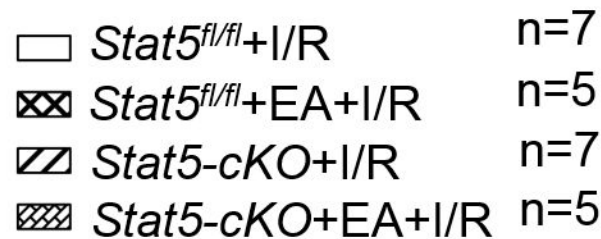
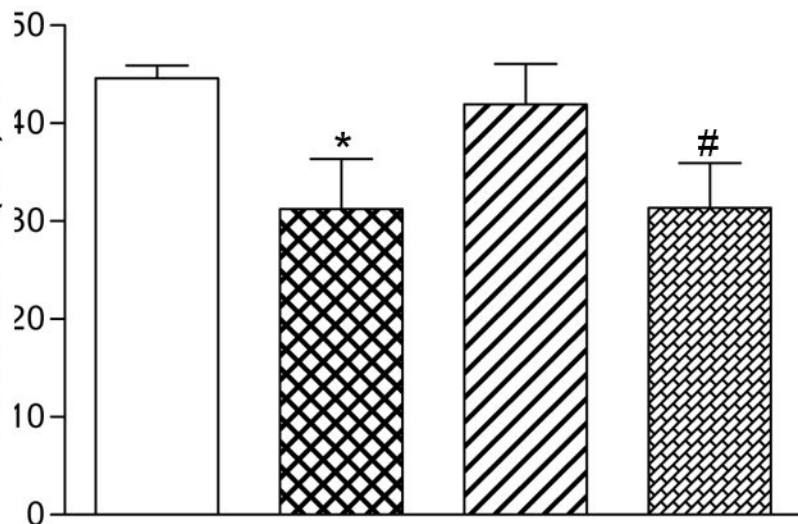
Arc	1.14086	20.7638	4.18587	Trim47	26.4865	6.40037	-2.04903
Agt	1.55521	27.442	4.1412	Tmsb10	110.513	26.7491	-2.04665
Rnd1	0.793702	12.8902	4.02154	B3gnt3	2.39685	0.580215	-2.04648
Pdk4	35.6426	578.857	4.02153	Myo7a	2.29499	0.574977	-1.99691
Plaur	1.59226	25.5567	4.00455	Fam181b	3.87361	0.976908	-1.98738

B. The top 30 differentially expressed genes obtained from comparing *Stat5-cKO*+EA+I/R vs.

Stat5-cKO+I/R

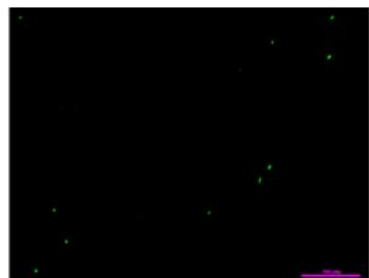
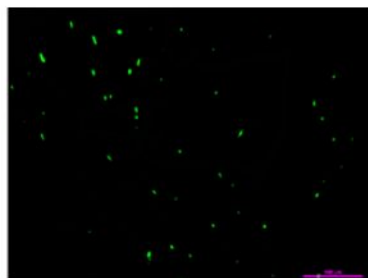
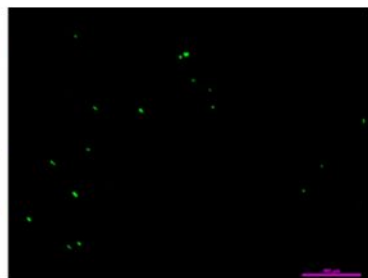
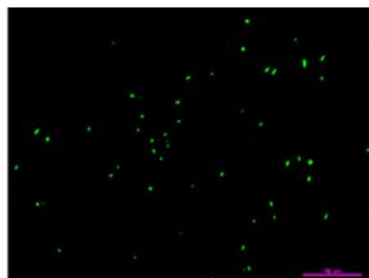
Up-regulated in EA against I/R				Down-regulated in EA against I/R			
Gene name	value_1	value_2	log2 (fold_change)	Gene name	value_1	value_2	log2 (fold_change)
Eno1b	0.503646	6.53728	3.69821	Olfr1033	855.24	3.24857	-8.04038
Dynlt1b	1.11668	14.442	3.69299	Gm45551	221.558	1.31604	-7.39534
H2-Q1	0.264109	3.03007	3.52015	Gm38271	30.2569	0.353232	-6.4205
Tmem181c-ps	0.99792	11.1342	3.47994	Psg16	2.41103	0.0719611	-5.06629
Gm4737	0.445121	4.58914	3.36595	Gm3365	7.26917	0.262255	-4.79275
2610005L07Rik	1.25086	12.1968	3.28551	Sugct	11.7515	0.52977	-4.47133
Gm14421	0.377049	3.17075	3.072	Gm43197	55.389	3.11501	-4.15229
Mmp3	0.379936	3.17412	3.06253	Gm15280	32.1097	2.05499	-3.96581
Gm42887	0.544175	4.41682	3.02087	CAAA01147332.1	97.5278	7.86365	-3.63254
Ubb	35.8823	290.433	3.01686	Zfp729a	6.97773	0.621896	-3.48801
Hba-a2	44.9947	363.254	3.01315	Adgra3	25.8651	3.26536	-2.98569
Tmem191c	0.28056	2.17679	2.95582	Fmod	3.18759	0.452927	-2.81512
Gdnf	0.160275	1.21115	2.91776	Dpy19l3	2.2277	0.347531	-2.68034
Rpl3-ps1	3.02696	22.6124	2.90117	Gm37324	1.86878	0.299513	-2.64141
Stbd1	0.465139	3.32577	2.83795	Gm48274	72.516	11.6454	-2.63854
Adh6b	0.422625	3.00224	2.82859	Pilra	3.10358	0.507	-2.61387
Hba-a1	78.1547	542.904	2.79629	Prc1	1.51292	0.247267	-2.6132
Polr2l	6.80429	43.8946	2.68952	Clec4e	6.2329	1.08171	-2.52658
Myh7	174.331	1091.89	2.64692	Spp1	3.08682	0.543414	-2.506
Gapdh	603.792	3577.93	2.567	Rac2	14.0493	2.49669	-2.49241
Pttg1	5.6626	32.9153	2.53922	Oxnad1	117.772	21.1786	-2.47532
Zc3h3	0.178519	1.03346	2.53333	Fggy	4.18537	0.772849	-2.4371

Gm6472	5.6958	31.1981	2.45349	Gm44215	2.03074	0.376049	-2.43301
Cys1	0.799506	4.37525	2.45218	Lars2	129.273	25.3961	-2.34774
Tgtp2	0.951374	5.16733	2.44134	Zfp975	3.23415	0.636673	-2.34476
Rps6	94.127	497.199	2.40114	Bace2	8.13204	1.6647	-2.28836
Hspa1a	20.8766	109.614	2.39248	Suds3	101.31	22.7191	-2.1568
Eif3j2	0.89728	4.63881	2.37012	Tesk1	11.7699	2.74535	-2.10004
Gm8116	1.05436	5.39728	2.35587	Insig2	86.0597	20.4798	-2.07113
Gm15459	34.4931	176.148	2.35241	Pnkp	30.3154	7.36189	-2.0419

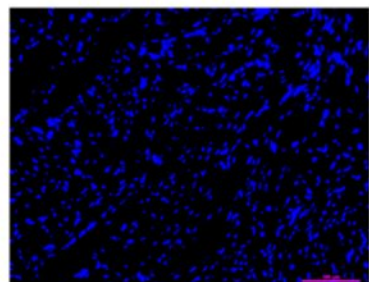
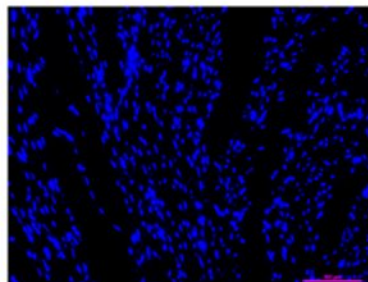
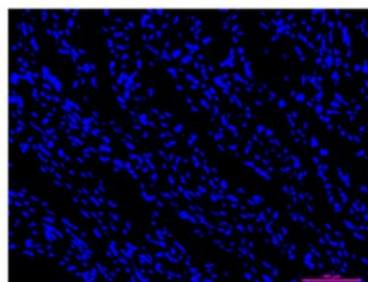
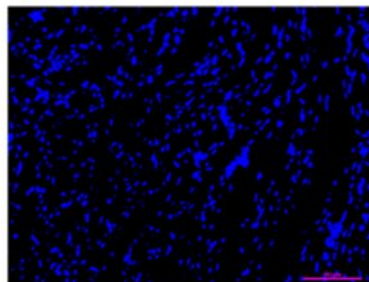
A*Stat5^{fl/fl}+I/R**Stat5-cKO+I/R**Stat5^{fl/fl}+EA+I/R**Stat5-cKO+EA+I/R***B**myocardial infarction sizes (IS)
/total area (TA) %

A*Stat5^{fl/fl}+I/R**Stat5^{fl/fl}+EA+I/R**Stat5-cKO+I/R**Stat5-cKO+EA+I/R*

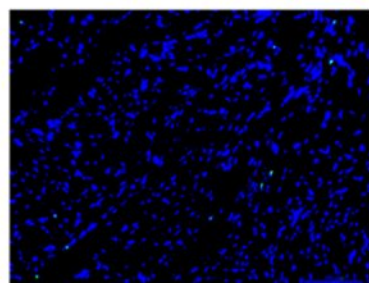
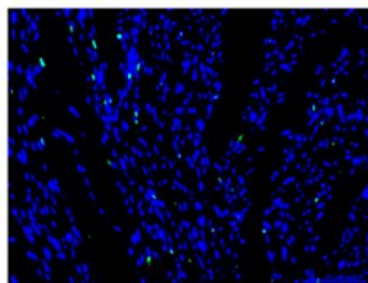
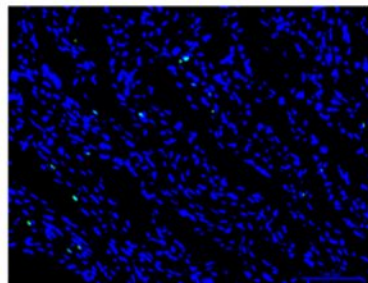
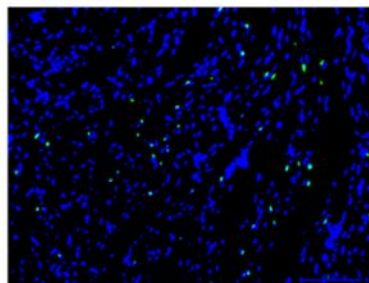
TUNEL

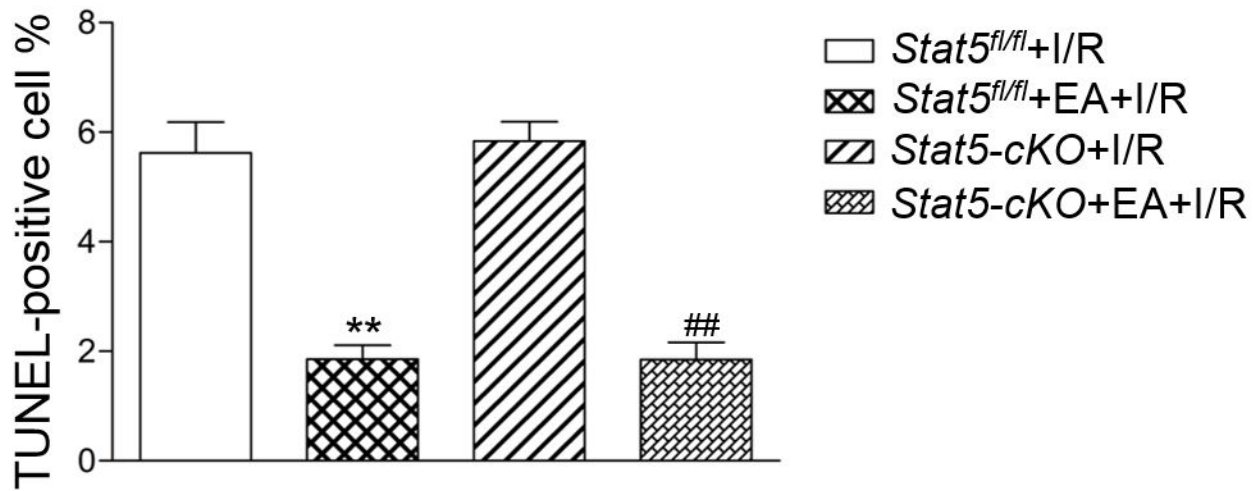


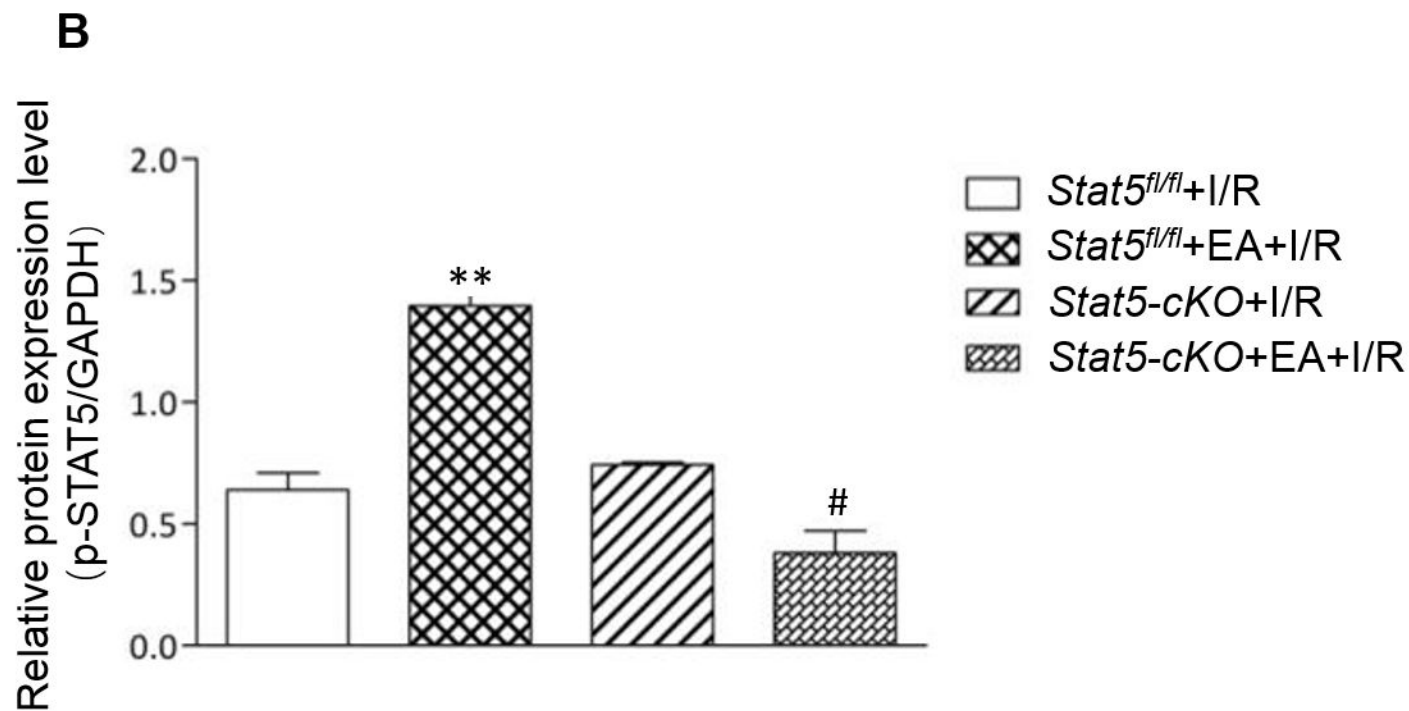
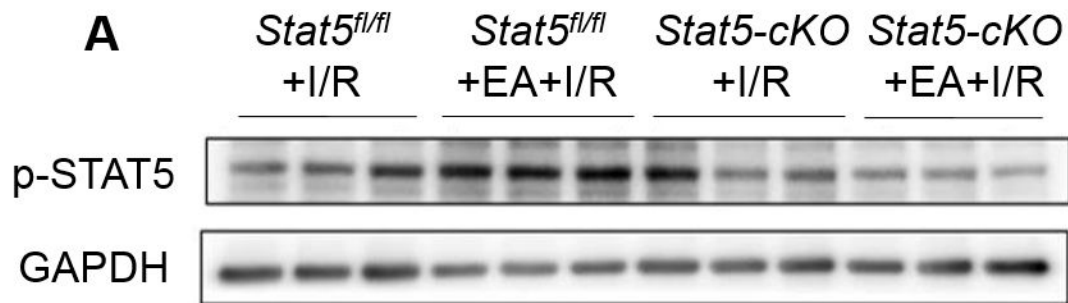
DAPI

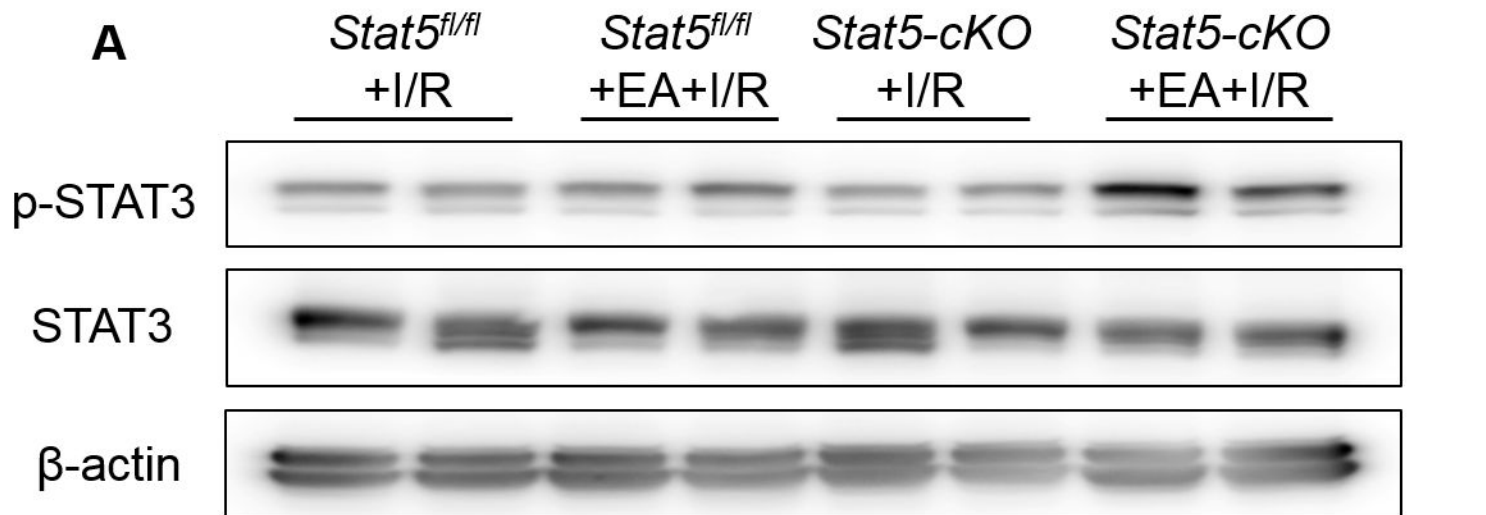


MERAGE

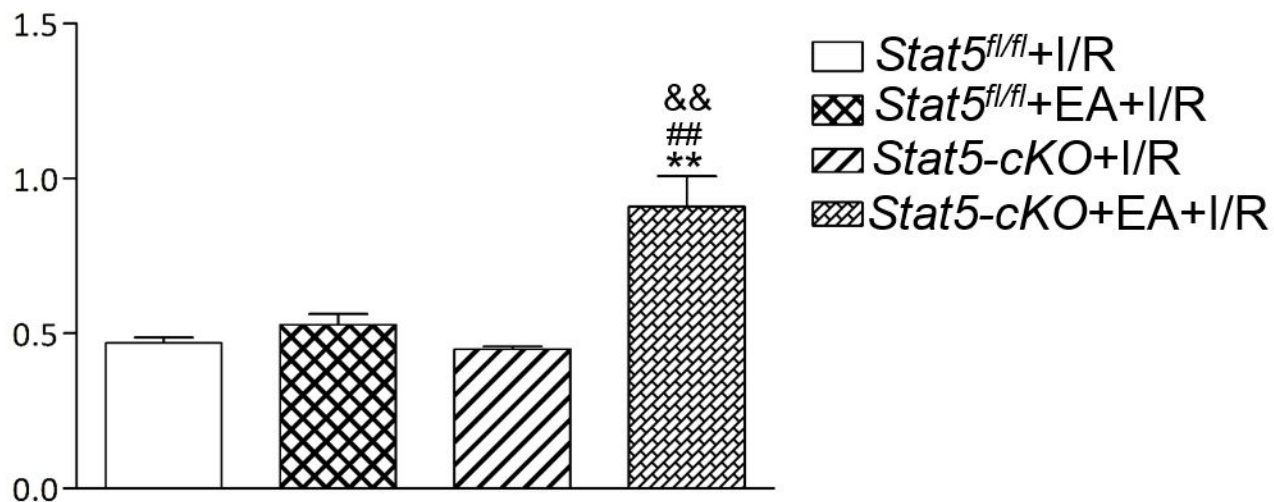


B



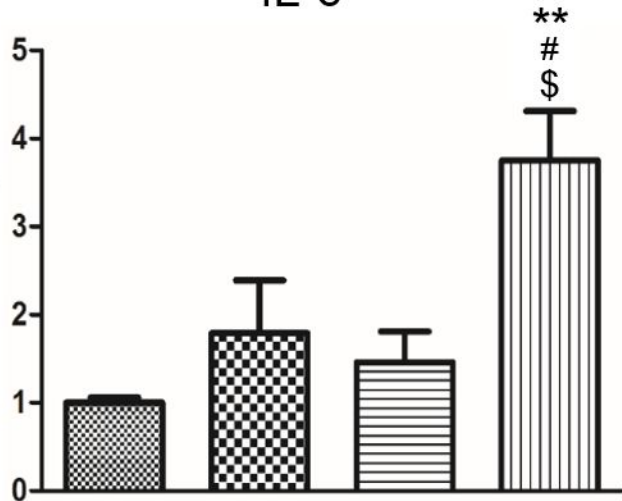


Relative protein expression levels
(p-STAT3/STAT3)

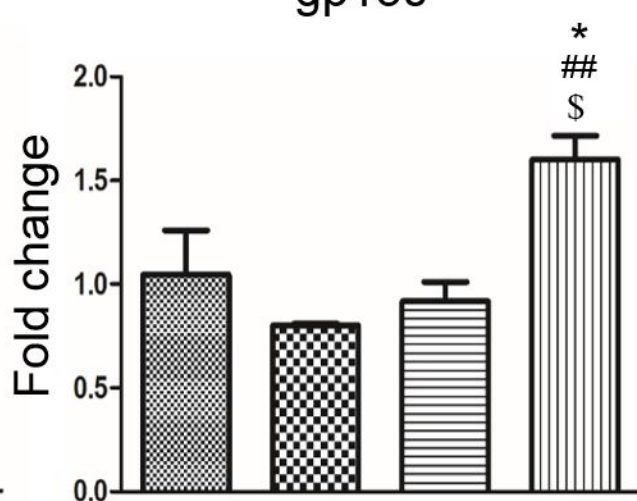






B

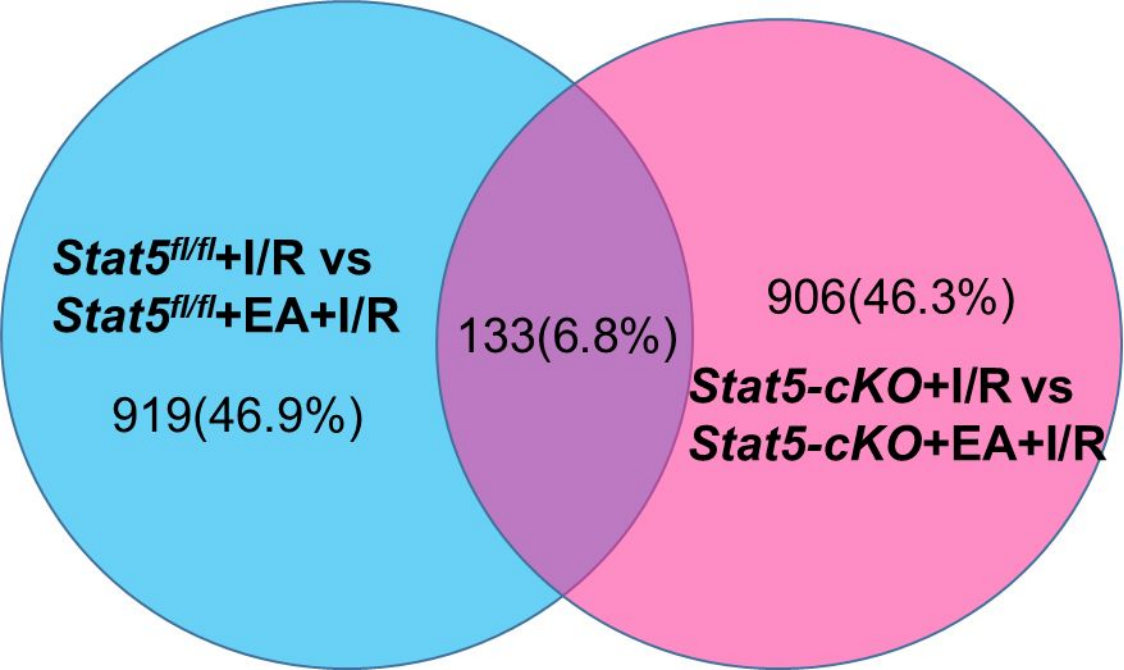
IL-6

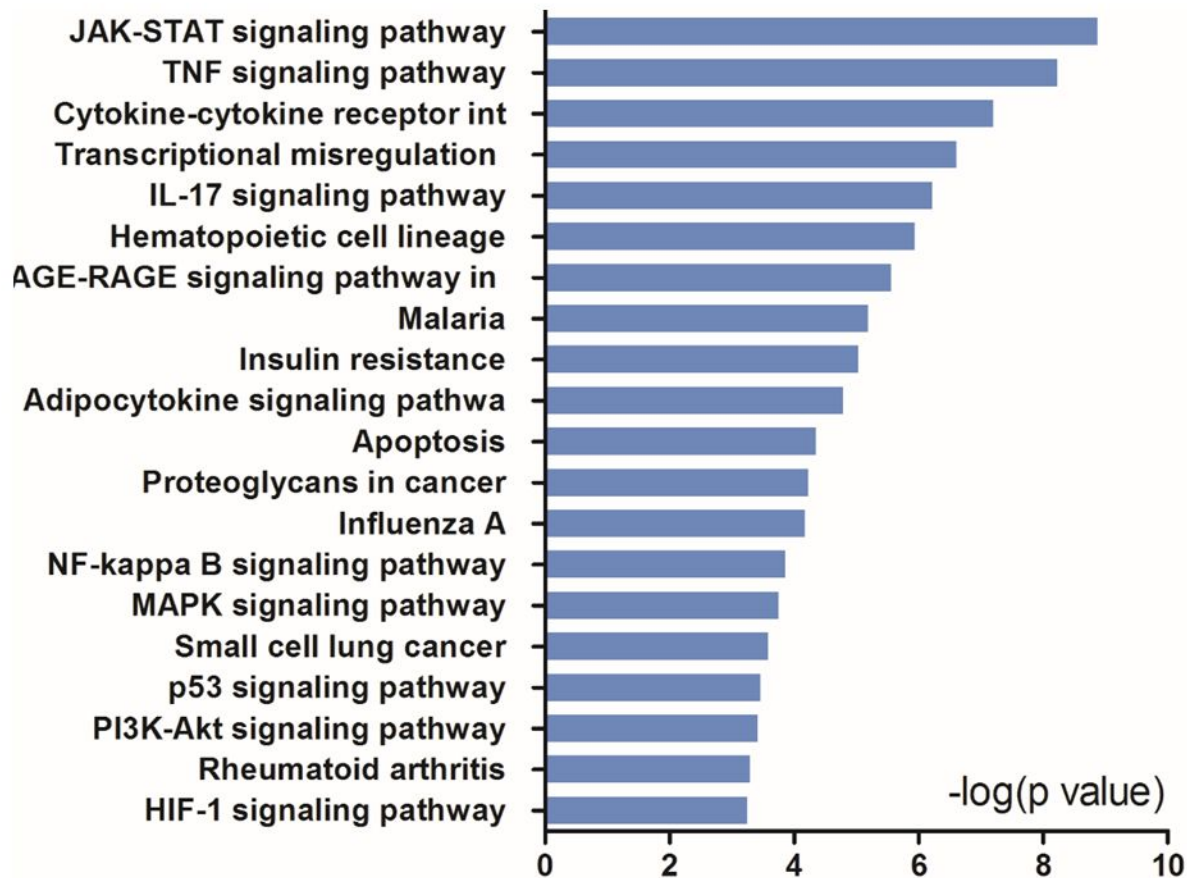


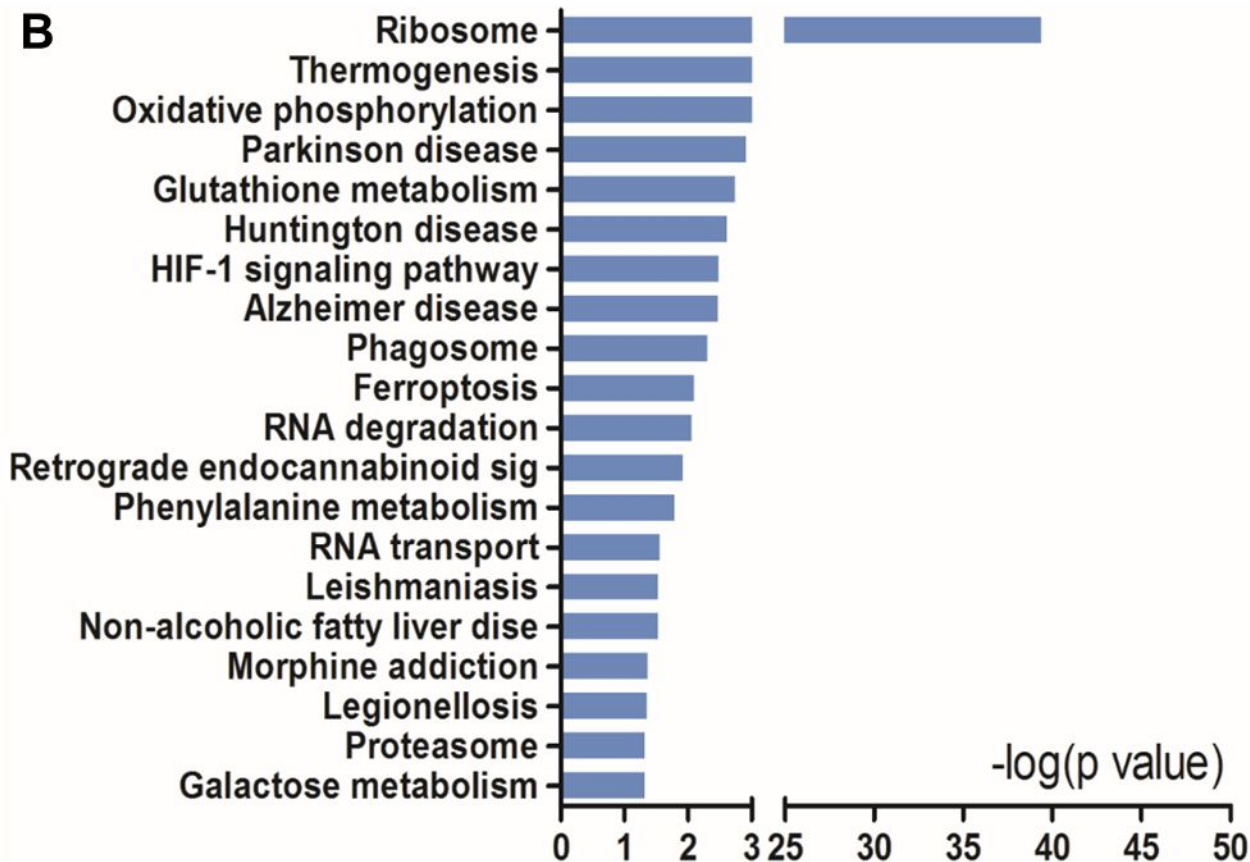
gp130

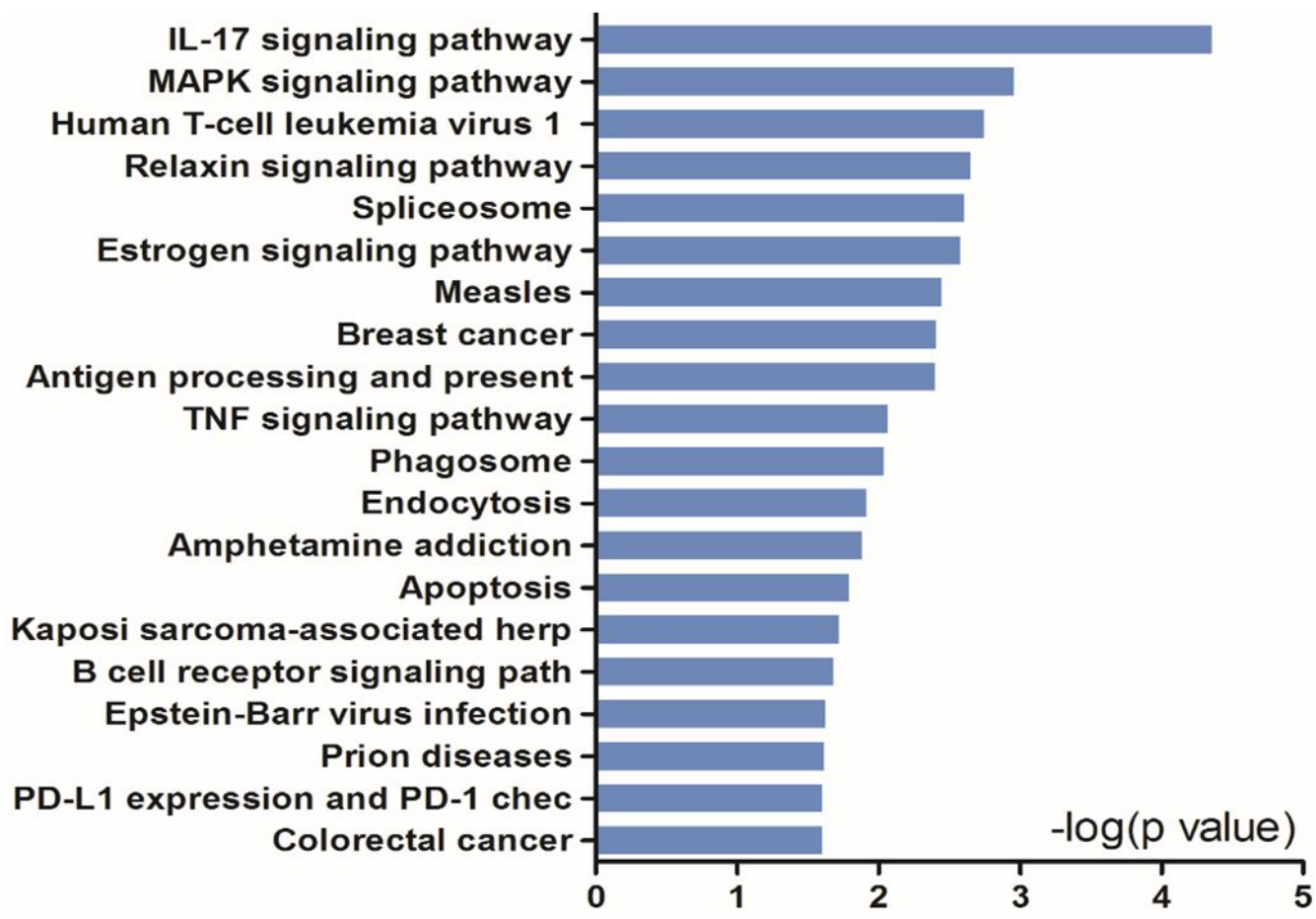


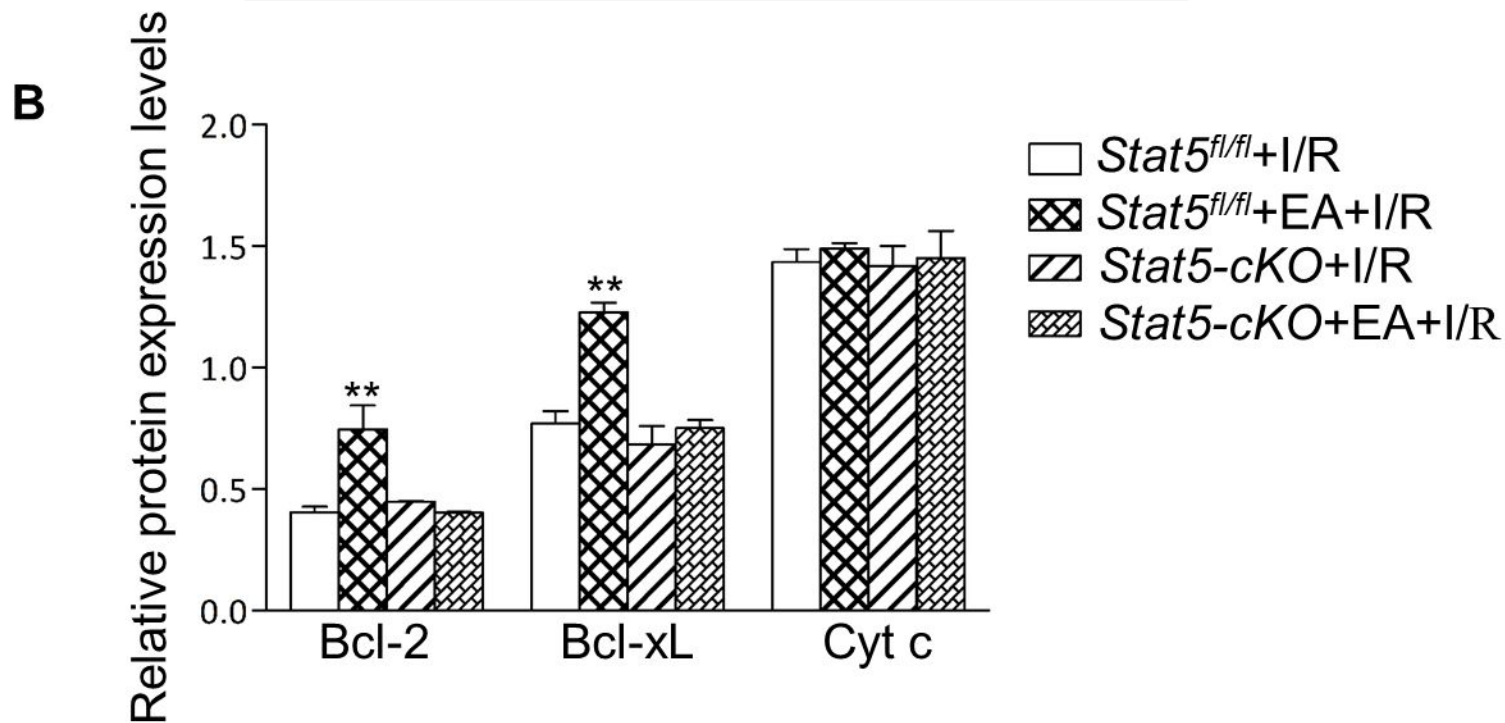
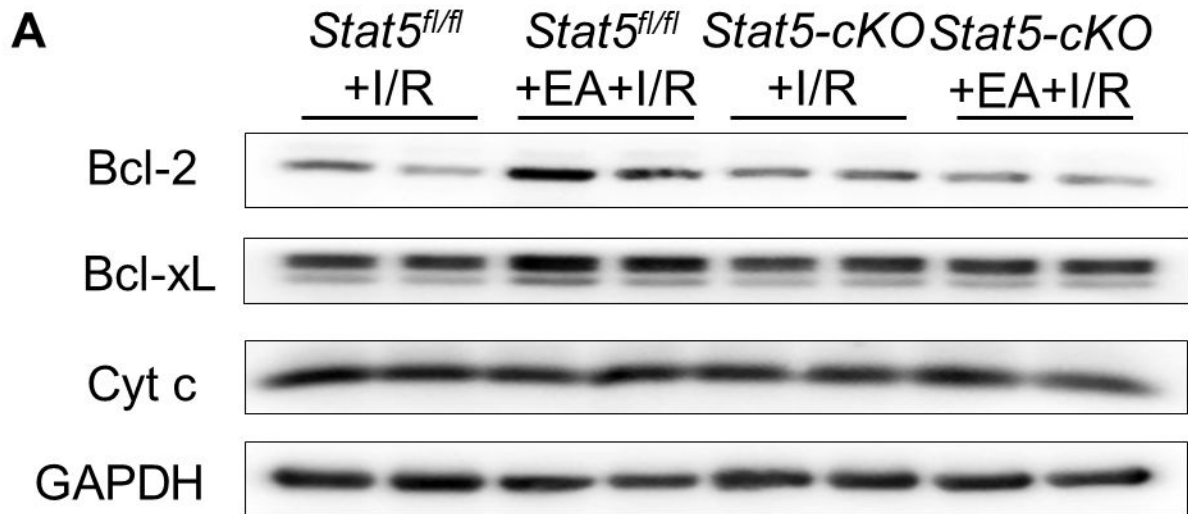
-  *Stat5^{fl/fl}+I/R*
-  *Stat5^{fl/fl}+EA+I/R*
-  *Stat5-cKO+I/R*
-  *Stat5-cKO+EA+I/R*

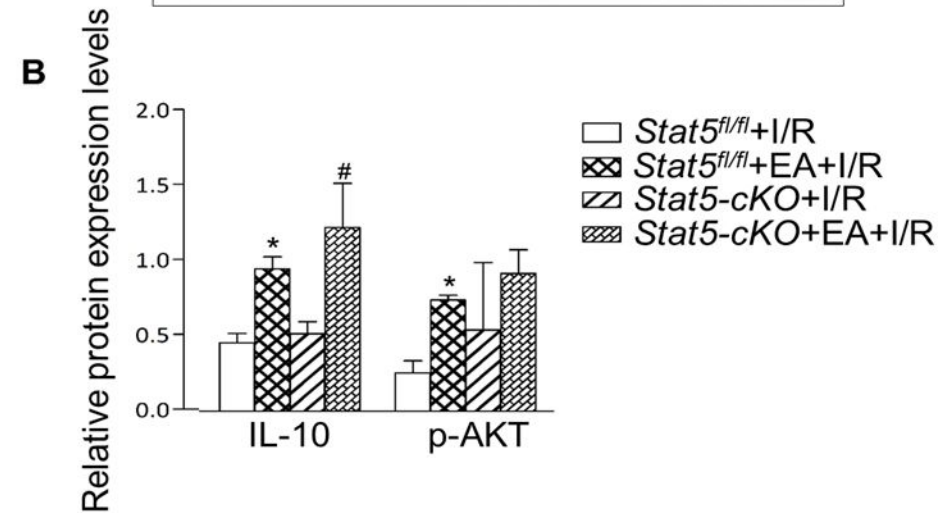
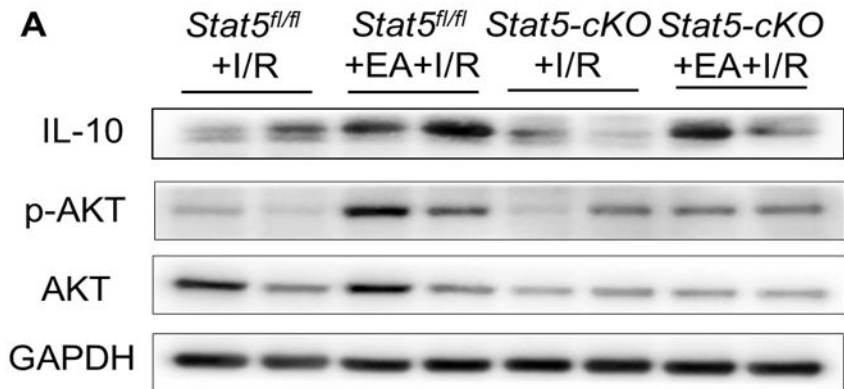


A

B

C





Stat5^{fl/fl} *Stat5^{fl/fl}* *Stat5⁻* *Stat5-cKO*
 +I/R +EA+I/R cKO+I/R +EA+I/R

